AMERICAN SOCIETY FOR MICROBIOLOGY | Journal of Bacteriology

De Novo Guanine Biosynthesis but Not the Riboswitch-Regulated Purine Salvage Pathway Is Required for *Staphylococcus aureus* Infection *In Vivo*

Eric M. Kofoed,[a] Donghong Yan,[b] Anand K. Katakam,[c] Mike Reichelt,[c] Baiwei Lin,[d] Janice Kim,[b] Summer Park,[b] Shailesh V. Date,[a] Ian R. Monk,[e] Min Xu,[b] Cary D. Austin,[c] Till Maurer,[d] Man-Wah Tan[a]

Infectious Diseases Department,[a] Translational Immunology Department,[b] Pathology Department,[c] and Structural Biology Department,[d] Genentech Inc., South San Francisco, California, USA; Department of Microbiology and Immunology, University of Melbourne at the Doherty Institute for Infection and Immunity, Melbourne, Australia[e]

ABSTRACT

***De novo* guanine biosynthesis is an evolutionarily conserved pathway that creates sufficient nucleotides to support DNA replication, transcription, and translation. Bacteria can also salvage nutrients from the environment to supplement the *de novo* pathway, but the relative importance of either pathway during *Staphylococcus aureus* infection is not known. In *S. aureus*, genes important for both *de novo* and salvage pathways are regulated by a guanine riboswitch. Bacterial riboswitches have attracted attention as a novel class of antibacterial drug targets because they have high affinity for small molecules, are absent in humans, and regulate the expression of multiple genes, including those essential for cell viability. Genetic and biophysical methods confirm the existence of a bona fide guanine riboswitch upstream of an operon encoding xanthine phosphoribosyltransferase (*xpt*), xanthine permease (*pbuX*), inosine-5′-monophosphate dehydrogenase (*guaB*), and GMP synthetase (*guaA*) that represses the expression of these genes in response to guanine. We found that *S. aureus guaB* and *guaA* are also transcribed independently of riboswitch control by alternative promoter elements. Deletion of *xpt-pbuX-guaB-guaA* genes resulted in guanine auxotrophy, failure to grow in human serum, profound abnormalities in cell morphology, and avirulence in mouse infection models, whereas deletion of the purine salvage genes *xpt-pbuX* had none of these effects. Disruption of *guaB* or *guaA* recapitulates the *xpt-pbuX-guaB-guaA* deletion *in vivo*. In total, the data demonstrate that targeting the guanine riboswitch alone is insufficient to treat *S. aureus* infections but that inhibition of *guaA* or *guaB* could have therapeutic utility.**

IMPORTANCE

***De novo* guanine biosynthesis and purine salvage genes were reported to be regulated by a guanine riboswitch in *Staphylococcus aureus*. We demonstrate here that this is not true, because alternative promoter elements that uncouple the *de novo* pathway from riboswitch regulation were identified. We found that in animal models of infection, the purine salvage pathway is insufficient for *S. aureus* survival in the absence of *de novo* guanine biosynthesis. These data suggest targeting the *de novo* guanine biosynthesis pathway may have therapeutic utility in the treatment of *S. aureus* infections.**

Riboswitches are structured noncoding RNA elements located in the 5′ untranslated regions (5′-UTR) of a mRNA molecule. These molecular switches are present in many biosynthetic operons in bacteria. Riboswitches consist of a small-molecule-binding aptamer and an expression platform that together control gene expression in *cis* by directly binding to small molecules. The riboswitch is one example of negative feedback that, in some cases, explains how the end product of a biosynthetic or nutrient salvage operon can directly inhibit its own expression. One of the best characterized are the purine riboswitches that control enzymes involved in *de novo* purine biosynthesis, nucleotide metabolism, and nucleotide transport. Ligand binding by the aptamer domain transduces information about nutrient concentration to the expression platform via conformational changes associated with the ligand bound state (1). Guanine binding to its cognate riboswitch causes transcriptional attenuation by formation of an intrinsic terminator (2). Thus, elevated cellular concentrations of nutrients will shut down expression of the cognate biosynthetic operon.

In the model Gram-positive bacteria *Bacillus subtilis*, expression of the two-gene purine salvage operon *xpt-pbuX* encoding xanthine phosphoribosyltransferase (*xpt*) and xanthine permease (*pbuX*) is tightly regulated by guanine concentration (1, 3, 4). Transcriptional regulation of purine biosynthesis by guanine has been linked to the presence of a guanine-binding riboswitch in the 5′-UTR, by the GTP-binding LacI-type repressor CodY, and the regulator PurR (4–6). In *Staphylococcus aureus*, the riboswitch at the 5′-UTR of the mRNA consisting of the four-gene operon *xpt-pbuX-guaB-guaA* (henceforth referred to as *xpt*-riboswitch) has been reported to regulate the expression of these genes in response

Received 13 January 2016 **Accepted** 5 May 2016

Accepted manuscript posted online 9 May 2016

Citation Kofoed EM, Yan D, Katakam AK, Reichelt M, Lin B, Kim J, Park S, Date SV, Monk IR, Xu M, Austin CD, Maurer T, Tan M-W. 2016. *De novo* guanine biosynthesis but not the riboswitch-regulated purine salvage pathway is required for *Staphylococcus aureus* infection *in vivo*. J Bacteriol 198:2001–2015. doi:10.1128/JB.00051-16.

Editor: O. Schneewind, The University of Chicago

Address correspondence to Eric M. Kofoed, kofoede@gene.com, or Man-Wah Tan, tan.man-wah@gene.com.

Supplemental material for this article may be found at http://dx.doi.org/10.1128/JB.00051-16.

to guanine (7, 8). Both *guaB* and *guaA*, which encode inosine-5′-monophosphate dehydrogenase and GMP synthetase, respectively, are required for *de novo* biosynthesis of guanine nucleotides.

Crystal structures of riboswitches bound to small-molecule nutrients and their analogs ignited great interest in the possibility of identifying selective and potent molecules that would shut off essential gene expression in pathogens (3, 4). Many high-affinity riboswitch-binding purine and lysine analogs have been discovered (3, 9), and *in silico* modeling efforts have expanded the arsenal of tool compounds (10). In some cases, biochemical and structural information about riboswitches and their cognate ligands is far more advanced than our knowledge of the underlying pathogen biology being targeted. Two encouraging advances in the field came with identification of the flavin mononucleotide (FMN) riboswitch as the target for the natural antibiotic roseoflavin (11), and the identification of 2,5,6-triaminopyrimidin-4-one (PC1) that bound the *xpt*-riboswitch and was bactericidal to *S. aureus in vivo* (7). These studies showed that the riboswitches have potential as targets of antibiotics, and that in certain infection models, ligand analogs can kill bacterial pathogens.

However, many large hurdles exist to developing antibiotics that target the riboswitch. These include an incomplete understanding of what genes are essential for individual pathogens *in vivo*, the difficulty in parsing on- and off-target effects of lead compounds, the cytoplasmic location of the target, and lack of sufficient validation and/or commercial availability for many published analogs. Nevertheless, we set out to test the hypothesis that a riboswitch could be a good therapeutic target. We focused on the purine riboswitches in *S. aureus* because they were predicted to regulate two essential gene clusters, the *xpt-pbuX-guaB-guaA* and *nrdI-nrdE-nrdF* operons (7, 12, 13).

MATERIALS AND METHODS

Compounds. 4-Hydroxy-2,5,6-triaminopyrimidine sulfate (PC1), guanine, adenine, hypoxanthine, xanthine, guanosine, 2-aminopurine, 2′-deoxyguanosine, 6-thioguanine, 2,4-diaminopyrimidine, 2,4,6-triaminopyrimidine, 2,6-diaminopurine, 2,4,5,6-tetraaminopyrimidine, 2-nitrophenyl β-D-galactopyranoside, and all common chemical reagents were obtained from Sigma. 2-Acetamido-6-hydroxypurine was obtained from TCI. The identity and purity of PC1 were verified in-house by liquid chromatography (LC) and mass spectrometry (MS). PC1 stock solutions (2 mg/ml) required 0.03 N NaOH and 1.5 mM dithiothreitol (DTT) to promote solubility and prevent oxidative self-condensation (7, 8). All other compounds were made as 100 mM stocks in 0.1 N NaOH.

Construction of pIMC85. The parental vector pIME6 was constructed by splicing by overhang extension PCR (SOE PCR; with primers IM202/IM205) joining the Pcp25-*ermB* marker (amplified with primers IM202/IM203 from pFX3EM) (57) to the partial replicon (*repB*; amplified with primers IM204/IM205) of pVE6007 (58). The SOE PCR product was gel extracted, phosphorylated with polynucleotide kinase, and self-ligated. The ligation was used to transform DC10B-R (EC10B [58] with the *dcm* gene deleted), and transformants were selected on L agar containing 200 μg/ml of erythromycin. DC10B-R supplies the RepA in *trans*, essential for plasmid replication. The soxR bidirectional transcription terminator was cloned as a double-stranded oligonucleotide into the unique BglII/EcoRI sites. The multiple-cloning site (MCS) was inserted between EcoRI and HindIII sites as a double-stranded oligonucleotide. To improve selection in diverse *S. aureus* strains, the Pcp25-*ermB* marker was exchanged for Phelp-*cat* (with an internal NcoI site deleted) amplified from pIMAY (with primers IM291/IM307/IM308/IM292) and was cloned into the unique SphI/NcoI sites, creating pIMC6. Genomic DNA was isolated from purified phage 85, and *attP* (amplified using primers IM285/IM286 and BglII/SphI restriction sites) and int (amplified using primers IM287/IM288 and NcoI/PstI restriction sites) were cloned to create pIMC85. The MCS is flanked by *soxR* and *tonB* transcription terminators, and phage 85 integrase is cotranscribed with the *cat* gene from the Phelp promoter. The plasmid cannot replicate in *S. aureus*; therefore, upon electroporation of the plasmid into the target strain, production of the Int stimulates stable plasmid integration between convergent genes *rpmF* and *isdB* (59). Transformants can be selected on brain heart infusion (BHI) agar with 10 μg/ml of chloramphenicol and screened by colony PCR with IM289/IM290.

Cloning. Clean unmarked deletions in *S. aureus* were generated by homologous recombination using the pIMAY vector (14), and stable integration between the *isdB-rpmF* phage 85 *att* site was achieved using the pIMC85 vector. For ease of genetic manipulation, we used as genetic background a strain in which the restriction modification enzymes have been deleted; this strain is indistinguishable from the parental wild-type (WT) strain in mouse infection models (Table 1) (14). Transcriptional reporter constructs were generated first by PCR cloning promoter fragments into the *B. subtilis* integration vector pDG1661 using EcoRI/BamHI sites upstream of *lacZ* and were stably integrated into the *amyE* locus of *B. subtilis* (1A771) as previously described (Bacillus Genetics Stock Center) (4). These fusion constructs were subcloned for integration into *S. aureus* by digestion with PflF1/EcoRI followed by Klenow fill-in and blunt-end ligation into SmaI-digested pIMC85, followed by stable integration.

Miller assay. Transcriptional reporter strains in *B. subtilis* were back diluted 1:100 from overnight cultures and grown to log phase in 1× *Bacillus* medium [14 g/liter K_2HPO_4, 6 g/liter KH_2PO_4, 2 g/liter $(NH_4)_2SO_4$, 1 g/liter Na_3 citrate·$2H_2O$, 1 g/liter yeast extract, 0.2g/liter Casamino Acids, 0.5% (wt/vol) glucose], optical density at 600 nm was measured, and 1 ml of cells pelleted and lysed in 1 ml of 1× Z-buffer plus 40 μl chloroform and 20 μl of 0.1% SDS, followed by the addition of 100 μl of chromogenic substrate *o*-nitrophenyl-β-d-galactopyranoside (ONPG) (4 mg/ml in Z-buffer) per sample. The time of reaction was recorded, stopped with 200 μl of 1 M Na_2CO_3, particulates were quickly spun out, absorbance at 420 nm was measured, and Miller units were calculated as described previously (15). Assays in *S. aureus* were performed as described below, but the specific growth medium used (tryptic soy broth, Mueller-Hinton II broth, or chemically defined medium [CDM]) is indicated in figure legends.

Chemically defined medium for growth of *S. aureus*. Chemically defined medium was formulated as previously described (16) for ZMB2 with the intentional exclusion of adenine, guanine, and xanthine.

Quantitative reverse transcription-PCR (qRT-PCR). Custom TaqMan gene expression assays were obtained from Applied Biosystems (Life Technologies) as primer and 6-carboxyfluorescein (FAM)/minor groove binder (MGB)-nonfluorescent quencher (NFQ) reporter/quencher probe sets. First-strand synthesis for RT-PCR was performed using SuperScript III reverse transcriptase (Invitrogen). Analysis of relative gene expression data was performed using Applied Biosystems software and the $2^{-\Delta\Delta C_T}$ method (17, 18).

Northern blotting. Northern blotting was performed by classic methods (19). In brief, total RNA was harvested from log-phase cultures using the TRIzol method (Ambion), size separated by denaturing PAGE, overnight capillary transferred to nylon membranes, UV cross-linked, and processed using the NorthernMax blotting kit (Life Technologies). Probe template DNA was PCR amplified off the pIMC85-*xpt-guaA* complementation plasmid (for *guaA* and *guaB*) or *S. aureus* genomic DNA (for *rrsA*), gel extracted, and radioactively labeled using random hexamers, [α-^{32}P]dCTP, and Klenow fragment to yield 250- to 500-bp DNA probes for the detection of *guaB*, *guaA*, and *rrsA* transcripts.

5′ rapid amplification of cDNA ends (5′-RACE). Mapping the transcriptional start site of *guaB* was performed essentially as described by the manufacturer of the kit (catalog no. 18374-058; Invitrogen). In brief, we harvested total RNA from log-phase cultures, performed first-strand syn-

TABLE 1 Bacterial strains used in this study

Bacterial species and strain	Strain designation[a]	Relevant genotype or other information[b]	Reference or source
S. aureus NRS384	WT	Δ*hsdR* Δ*sauUSI*	14
B. subtilis 1A771	EK1	*amyE*::pDG1661-*B. subtilis xpt*(−305)-*lacZ*	This work[c]
B. subtilis 1A771	EK2	*amyE*::pDG1661-*S. aureus xpt*(−452)-*lacZ*	This work
S. aureus NRS384	EK3	Δ*hsdR* Δ*sauUSI* ϕ85*att*::pIMC85-*S. aureus xpt*(−452)-*lacZ*	This work
S. aureus NRS384	EK4	Δ*hsdR* Δ*sauUSI* ϕ85*att*::pIMC85-*S. aureus pbuX*(−568)-*lacZ*	This work
S. aureus NRS384	EK5	Δ*hsdR* Δ*sauUSI* ϕ85*att*::pIMC85-*S. aureus guaB*(−112)-*lacZ*	This work
S. aureus NRS384	EK6	Δ*hsdR* Δ*sauUSI* ϕ85*att*::pIMC85-*S. aureus guaA*(−414)-*lacZ*	This work
S. aureus NRS384	EK7	Δ*hsdR* Δ*sauUSI* ϕ85*att*::pIMC85-*S. aureus guaA*(−764)-*lacZ*	This work
S. aureus NRS384	EK8	Δ*hsdR* Δ*sauUSI* Δ*xpt-pbuX*	This work
S. aureus NRS384	EK9	Δ*hsdR* Δ*sauUSI pbuX*::Tn^{ERM}	This work
S. aureus NRS384	EK10	Δ*hsdR* Δ*sauUSI* Δ*xpt-pbuX-guaB-guaA*	This work
S. aureus NRS384	EK11	Δ*hsdR* Δ*sauUSI* Δ*xpt-pbuX-guaB-guaA* ϕ85*att*::pIMC85-*xpt-pbuX-*guaB-guaA*	This work
S. aureus NRS384	EK12	Δ*hsdR* Δ*sauUSI* Δ*xpt-pbuX-guaB-guaA* ϕ85*att*::pIMC85-*xpt-pbuX-guaB-*guaA*	This work
S. aureus NRS384	EK13	Δ*hsdR* Δ*sauUSI* Δ*guaB*	This work
S. aureus NRS384	EK14	Δ*hsdR* Δ*sauUSI* Δ*xpt-pbuX-guaB-guaA* ϕ85*att*::pIMC85-*xpt-pbuX-guaB-guaA*	This work
S. aureus NRS384	EK15	Δ*hsdR* Δ*sauUSI* ϕ85*att*::pIMC85-*S. aureus nrdI*(−218)-*lacZ*	This work
B. subtilis 1A771	EK16	*amyE*::pDG1661-*S. aureus nrdI*(−218)-*lacZ*	This work
K. pneumoniae subsp. *pneumoniae* Trevisan		ATCC 132	ATCC
E. faecalis OG1RF		ATCC 47077	ATCC
E. coli		Max Efficiency DH5α competent cells	Invitrogen
S. epidermidis Evans		ATCC 14990	ATCC

[a] Strain designations used in this study.
[b] The relevant genotype is given for the *S. aureus* and *B. subtilis* strains. An asterisk indicates introduction of an engineered stop codon in the gene. For the other species, the ATCC strain or product name is given.
[c] Reproduction of strain originally reported in Mandal et al. (4) and studied here.

thesis (Invitrogen), added a homopolymeric tail using terminal deoxynucleotidyltransferase, performed sequential nested PCRs, and TA-cloned products into the TOPO vector for sequence identification.

Water-LOGSY NMR. The direct binding interaction of guanine/adenine with the riboswitch was monitored using the water-LOGSY (water-ligand observed via gradient spectroscopy) method first described by Dalvit et al. (20). The inherent low density of protons in RNA macromolecules makes ligand binding detection using the bulk solvent water polarization more amenable than direct proton polarization using saturation transfer difference (STD) nuclear magnetic resonance (NMR) (21). All NMR experiments were performed on a Bruker Avance 600-MHz spectrometer using a 5-mm TXI cryoprobe set to the previously calibrated temperature of 284 K. Samples were measured in 3-mm NMR tubes (Wilmad, MA, USA) with a sample volume of 180 μl. The phosphate-buffered saline (PBS) solution contained 5% ^2H_2O and was adjusted to pH 7.2 using a standard glass electrode with no correction for deuterium isotope effects. The guanine riboswitch was at a concentration of 10 μM, and the ligands were added from stock solutions to a concentration of 500 μM.

Transmission electron microscopy. All samples were first fixed in modified Karnovsky's fixative (2% paraformaldehyde and 2.5% glutaraldehyde in 0.1 M sodium cacodylate buffer [pH 7.2]) and then postfixed in 1% aqueous osmium tetroxide for 2 h followed by incubation in 0.5% uranyl acetate for 2 h. The samples were then dehydrated through a series of ethanol solutions (50%, 70%, 90%, 95%, and 100%) followed by propylene oxide (each step was for 15 min) and embedded in Eponate 12 (Ted Pella, Redding, CA). Ultrathin sections (80 nm) were cut with an Ultracut microtome (Leica), stained with 0.2% lead citrate, and examined in a JEOL JEM-1400 transmission electron microscope (TEM) at 120 kV. Digital images were captured with a GATAN Ultrascan 1000 charge-coupled-device (CCD) camera. Quantification of morphological structures was performed manually in Microsoft PowerPoint by scoring for the presence of normal or abnormal septum on three 2,000× fields from each sample excluding cells with a diameter of <0.75 μm to avoid plane-of-sectioning artifacts. Quantification of external matrix thickness was performed on at least 12 independent 40,000× images by drawing a line between the cell membrane and the outermost staining of the cell wall, at two places on each cell. The average length was converted to nanometer values based on the proportion to the index included on each image. Data are presented as means ± standard errors of the means (SEM) for all TEM graphical representations.

Testing the virulence of bacterial mutants in mouse infection models. For mouse bacteremia model, 7-week-old A/J female mice (Jackson Lab) were infected through tail vein injection with 2E6 CFU different bacterial strains prepared from tryptic soy broth (TSB) log-phase culture. At days 1 and 3 postinfection, kidneys from infected mice were collected and homogenized for CFU determination on blood agar plates. For a neutropenic thigh infection model, neutropenia in 6-week-old CD1 female mice (Charles River Laboratory) was induced by injecting the mice with 150 mg of cyclophosphamide/kg of body weight and 100 mg of cyclophosphamide/kg intraperitoneally (i.p.) at days −5 and −2, respectively. At day 0, mice were inoculated with 50 μl bacteria per mouse containing 2E5 CFU in the thigh muscle. At 24 h postinfection, thigh muscle was collected and homogenized for CFU determination on blood agar plates.

RESULTS

***S. aureus* contains a guanine-responsive *xpt*-riboswitch.** *De novo* guanine biosynthesis creates sufficient nucleotides to support fundamental cellular processes, and bacteria also have the ability to salvage nutrients from the environment to supplement the *de novo* pathway (Fig. 1a). Interestingly, in *S. aureus*, the *xpt-pbuX-guaB-guaA* operon is a cluster of two salvage pathway genes (*xpt* and *pbuX*) and two *de novo* biosynthetic genes (*guaB* and *guaA*) that are regulated by a guanine riboswitch (Fig. 1b) (7). Primary sequence alignments of the minimal aptamer domain of

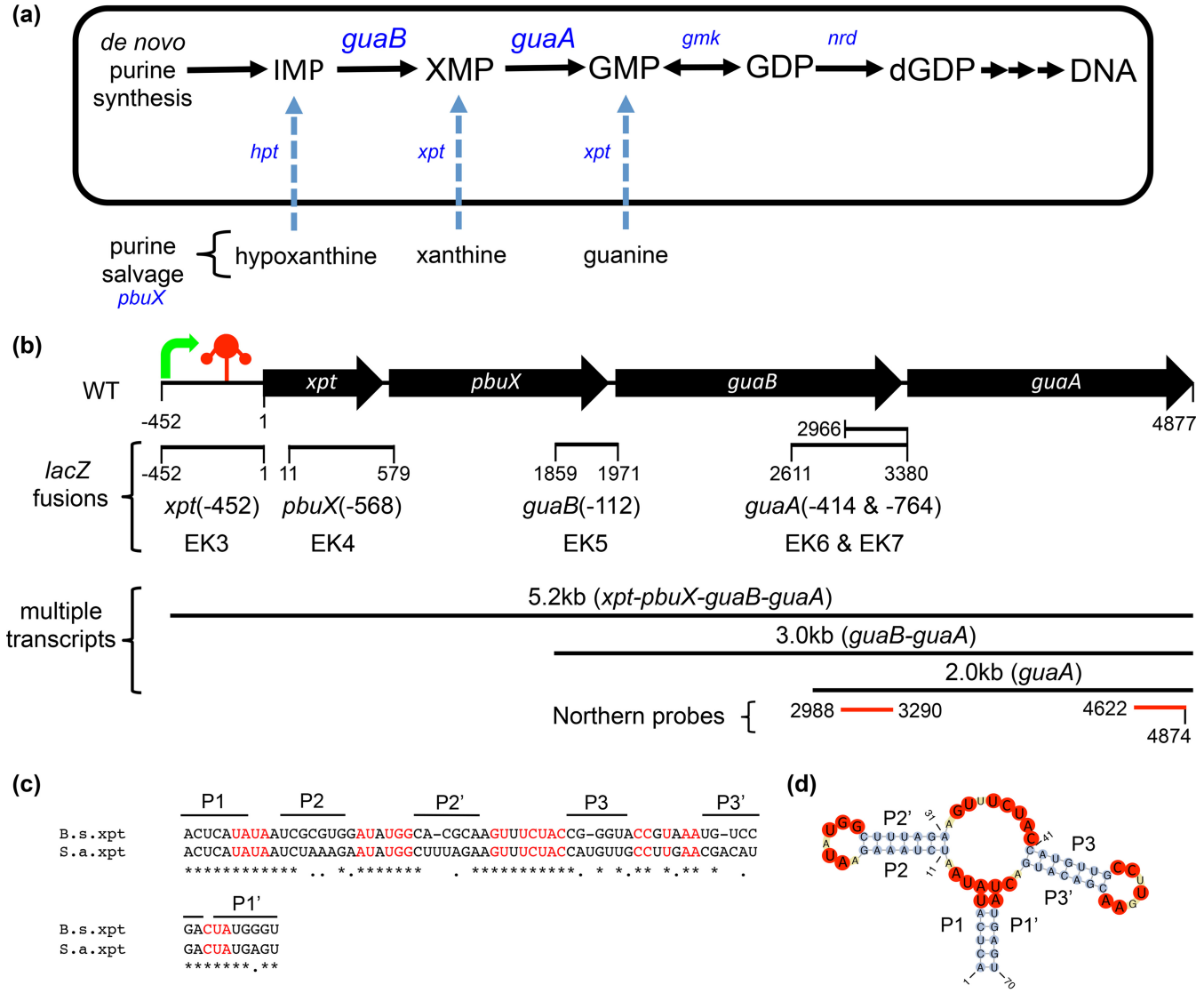

FIG 1 Guanine nucleotide biosynthetic pathway and the *xpt-pbuX-guaB-guaA* genetic locus in *Staphylococcus aureus*. (a) Schematic of the *de novo* guanine nucleotide biosynthesis and purine salvage pathways functional in *S. aureus*. IMP is the branch point for guanine and adenine *de novo* biosynthesis. IMP dehydrogenase (*guaB*) converts IMP to XMP and is the first committed and rate-limiting step in the pathway to dGTP used in DNA synthesis. IMP, XMP, and GMP can also be derived from the salvage of nucleosides and nucleobases using xanthine permease (*pbuX*) and hypoxanthine or xanthine phosphoribosyltransferases (*hpt* or *xpt*). GMP synthetase (*guaA*) is a glutamine amidotransferase that converts XMP to GMP, after which GMP kinase (*gmk*) and ribonucleotide reductases (*nrdIEF*) generate dGDP. (b) Organization of the *xpt-pbuX-guaB-guaA* gene locus in *S. aureus* showing open reading frames (black arrows), transcriptional start site (green arrow), and the riboswitch (red three-stem junction) located in the *xpt* 5′ untranslated region. Numbered segments from the *xpt* translational start codon represent the positions of different *lacZ* fusions made to interrogate alternative promoter elements within the locus, and the numbers in parentheses indicate the distance in base pairs upstream from the individual gene translational start sites. Alternative *guaB-guaA* and *guaA* transcripts identified by Northern blotting and reporter studies are indicated schematically with the observed size in kilobases, and message content in parentheses. The red bars indicate *guaB* and *guaA* probe positions used in Northern blotting. (c) Pairwise sequence alignment of the minimal aptamer domain of *B. subtilis* (B.s.) and *S. aureus* (S.a.) *xpt*-riboswitches highlighting (in red) conservation of nucleotides present in known guanine-binding riboswitch aptamers (4, 22). Black bars indicate the locations of the three (P1 to P3) pairing stems of the guanine riboswitch (4). (d) Predicted secondary structure of the *S. aureus xpt*-riboswitch aptamer showing the three-junction stem-loop structure typical of the purine riboswitch aptamer (56). Nucleotides are highlighted to show stem (blue), loop (yellow), and bases conserved in guanine-binding riboswitches (red) (4, 22).

the *xpt*-riboswitch from *B. subtilis* and *S. aureus* revealed high overall conservation and complete conservation of nucleotides that define the guanine-binding riboswitch aptamer (Fig. 1c) (4, 22). Secondary structure prediction of the *S. aureus xpt*-aptamer domain revealed similar stem-loop architecture as that found in *B. subtilis* (Fig. 1d). To determine whether the predicted *S. aureus* riboswitch functioned similar to the *B. subtilis* riboswitch, we first tested it in *B. subtilis* where the function was well characterized (4).

To test whether the *S. aureus xpt*-riboswitch was responsive to guanine, we fused the *xpt*-riboswitch upstream of *lacZ* to report the effects of purine ligands and analogs on gene expression as described previously (4). Reporters were stably integrated into the *amyE* locus of *B. subtilis* (Table 1). Both *B. subtilis* (EK1) and *S.*

aureus (EK2) xpt-5′-UTR-riboswitch *lacZ* reporters were completely turned off by guanine at 250 μM (Fig. 2a and b, respectively), confirming published *B. subtilis* data (3, 4), and indicating that the *S. aureus xpt*-leader sequence is guanine responsive. Because the *B. subtilis* riboswitch binds other purines with different affinities *in vitro* (3, 4), we tested hypoxanthine, adenine, and xanthine in the reporter assay. None of the other purines were as potent as guanine (Fig. 2c and d). Because both purine and pyrimidine analogs are capable of forming the proper network of hydrogen bonds to drive ligand-aptamer complex formation (3, 7, 23), a variety of purine and pyrimidine analogs were tested for their effect on reporter activity. Only 2-acetamido-6-hydroxypurine was as potent as guanine, suggesting that the *xpt*-riboswitch binds purine but not pyrimidine analogs (see Fig. S1a to d in the supplemental material).

The reporter system showed that in *B. subtilis*, the *S. aureus xpt*-riboswitch behaves similarly to the *B. subtilis xpt*-riboswitch, but this heterologous system may not accurately reflect the compound accessibility or the repertoire of transcriptional activators and repressors in *S. aureus*. Therefore, we stably integrated the *S. aureus xpt*(−452)-riboswitch reporter (an *xpt* riboswitch reporter construct starting at position −452 from the translational start site fused to the *lacZ* gene) into the *isdB-rpmF* phage 85 *att* site of NRS384, a virulent clinical isolate of *S. aureus*, to generate strain EK3 and tested the responses to natural purines and purine analogs. As expected, the *S. aureus xpt*-riboswitch reporter activity was strongly repressed in response to guanine (Fig. 2e). Interestingly, guanosine, 2′-deoxyguanosine, and 2-acetamido-6-hydroxypurine were equally effective at repression of reporter gene expression, whereas adenine significantly increased reporter expression (Fig. 2e). In contrast to the activity in *B. subtilis*, the *S. aureus* stable reporter strain had a modest but significant response to hypoxanthine, xanthine, and 2-aminopurine (Fig. 2e). While 2-acetamido-6-hydroxypurine has been shown biochemically to directly bind the guanine riboswitch (3), the other active compounds may be converted to guanine in the cell or may affect the balance of activators and repressors on the *xpt* promoter. Interestingly, we found that the *B. subtilis xpt*-riboswitch reporter was completely inactive in *S. aureus* (see Fig. S2 in the supplemental material). This observation emphasizes the need to interpret reporter data with caution, as small-molecule metabolites may have pleiotropic effects on the activity of transcriptional activators and repressors independent of the riboswitch, and heterologous systems may not accurately reflect the normal repertoire of regulators (24).

Confident that the *S. aureus xpt*-riboswitch was responsive to guanine *in vivo*, we then wanted to show directly whether guanine binding to the aptamer could explain this regulation. We used water-LOGSY NMR spectra to measure direct binding of purified RNA aptamers to the natural purines guanine and adenine (Fig. 2f). Both the *B. subtilis* and *S. aureus xpt*-riboswitch aptamers bound guanine but not adenine, 2-aminopurine, nor glucose (Fig. 2f and data not shown). These data confirm that the *xpt*-riboswitch from *S. aureus* directly bound ligands and repressed gene expression similarly to its *Bacillus xpt*-riboswitch orthologue (4, 22).

Repression of *xpt*, *pbuX*, *guaB*, and *guaA* expression by guanine. We then asked whether endogenous transcripts for *xpt*, *pbuX*, *guaB*, and *guaA* were reduced when *S. aureus* was grown in the presence of exogenous guanine. *S. aureus* grown in chemically defined medium (CDM) supplemented with 1 mM guanine led to a significant reduction of all four transcripts as measured by qRT-PCR, but we observed a surprising difference in the extent of guanine repression between *xpt-pbuX* and *guaB-guaA* (Fig. 3a). While there was an ~5-fold repression of *xpt* (0.29 ± 0.01, $P < 0.001$) and *pbuX* (0.22 ± 0.004, $P < 0.001$) in the presence of guanine, *guaB* (0.54 ± 0.09, $P = 0.014$) and *guaA* (0.62 ± 0.08, $P = 0.015$) message were reduced only ~2-fold compared to untreated *S. aureus* cultures (Fig. 3a). The extent of repression of *guaB* did not differ significantly from *guaA* ($P = 0.33$), but it was significantly different from *xpt* ($P = 0.01$) and *pbuX* ($P = 0.004$). Using four-fold-less guanine (250 μM), there was significant repression of *xpt* (to 0.26 ± 0.09 of untreated, $P = 0.008$) and *pbuX* (0.19 ± 0.07, $P = 0.004$), whereas *guaB* and *guaA* transcription was not affected by this concentration of guanine (Fig. 3b).

In log-phase *S. aureus*, Northern blots using probes specific for *guaB* and *guaA* RNA showed an abundance of a 3-kb message that corresponds to a major *guaB-guaA* bicistronic transcript, a 2-kb message corresponding to *guaA* message (Fig. 3c and d), and an extremely faint 5.2-kb message, visible only on very overexposed blots, that corresponds to the previously described *xpt-pbuX-guaB-guaA* transcript (Fig. 3c) (7). Neither *guaB* nor *guaA* message was detected in RNA extracted from *S. aureus* Δ*xpt-guaA* that confirmed probe specificity. RNA from the *S. aureus* Δ*xpt-pbuX* internal deletion retained the *guaB-guaA* alternative promoter and both the 3-kb *guaB-guaA* message and the 2-kb *guaA* message (Fig. 3c). Ethidium bromide staining and reprobing blots for ribosomal 16S RNA (*rrsA*) show equal loading of total RNA (Fig. 3c). Together, these results suggest the presence of alternative promoters that drive endogenous expression of *guaB* and *guaA* genes independent of the *xpt-pbuX* promoter and the *xpt*-riboswitch in *S. aureus*.

Identification of alternative promoters for *guaB* and *guaA*. To identify whether alternative promoters exist for *guaB* and/or *guaA* that are separate from the *xpt* riboswitch-controlled promoter, we constructed promoter-*lacZ* fusions by cloning regions upstream of each translational start site for *S. aureus pbuX*(−568) (EK4), *guaB*(−112) (EK5), and *guaA*(−414 and −764) (EK6 and EK7), and stably integrated these reporters into the *isdB-rpmF* phage 85 *att* site of *S. aureus* to directly compare promoter activity against *xpt*(−452) (EK3) (Fig. 1b and Table 1). While the *xpt*(−452) reporter strain was active and repressed by guanine, we failed to detect β-galactosidase activity from the *pbuX*(−568) reporter, suggesting the absence of an independent *pbuX* promoter within the test region. Consistent with the qRT-PCR results, the *guaB*(−112) reporter (EK5) was strongly active and was not regulated by guanine (Fig. 3d). Interestingly, the *guaA*(−764) reporter (EK7) was much stronger than either *guaB* or *xpt* promoters and not regulated by guanine, whereas the *guaA*(−414) reporter (EK6) was not active in *S. aureus*, thus locating an additional functional guanine-independent promoter for *guaA* between positions −764 and −414 (Fig. 3d). The presence of an alternative *guaA* promoter located within the *guaB* open reading frame is supported by the observation of a 2.0-kb *guaA* message that was detected by both *guaA*- and *guaB*-specific probes by Northern blotting (Fig. 3c). Together, our data suggest that the polycistronic *xpt-pbuX-guaB-guaA* message described previously (7) is a minor species in *S. aureus*, whereas the *guaB-guaA*(−112), and *guaA*(−764) alternative promoters are functionally dominant in *S. aureus* during active growth.

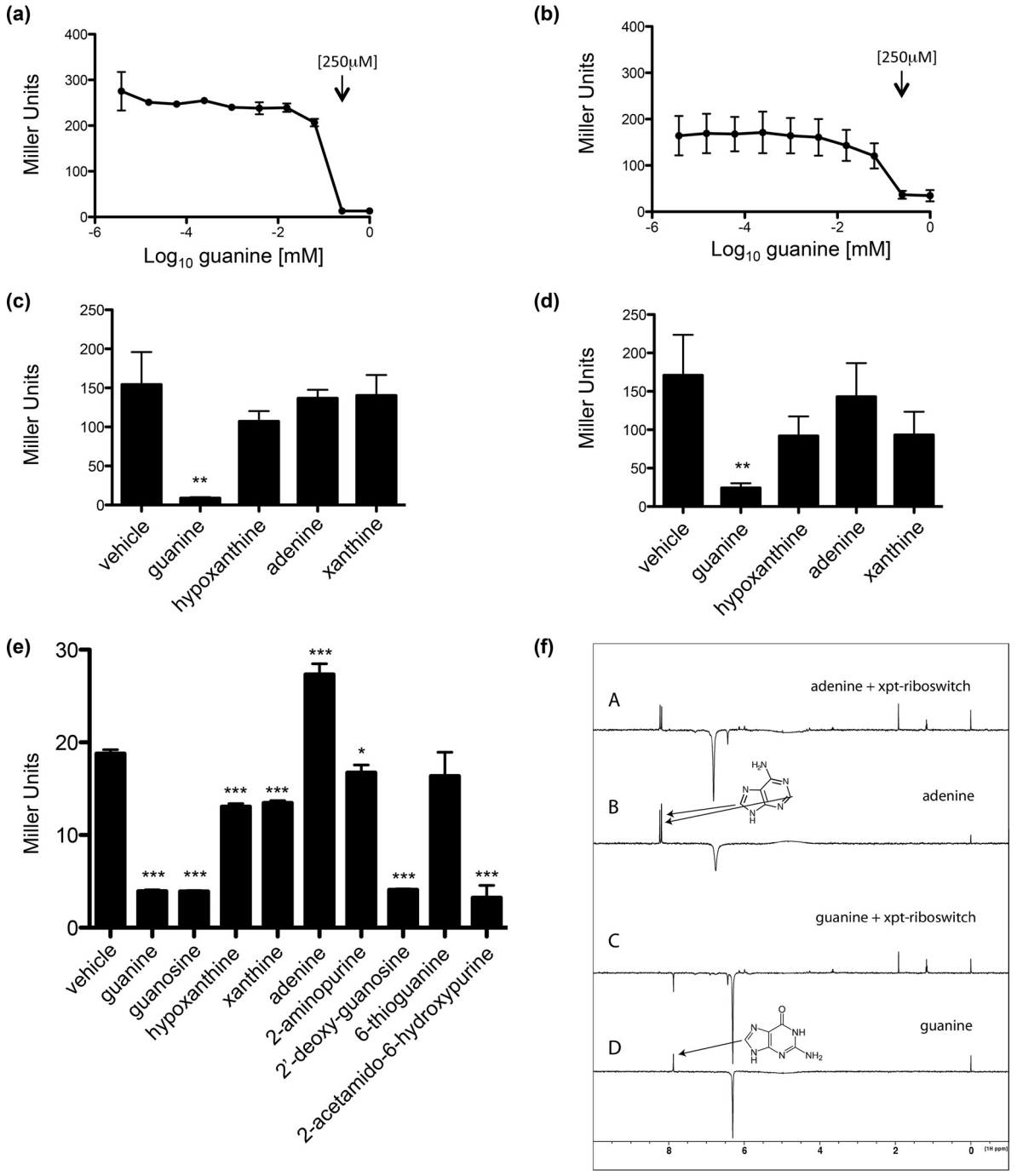

FIG 2 *S. aureus* contains a bona fide guanine riboswitch in the 5′-UTR of *xpt*. (a to d) Riboswitch transcriptional reporters were generated by fusing the *xpt* 5′-UTR riboswitch from *B. subtilis* (EK1) and *S. aureus* (EK2) to *lacZ* and integrated into the *amyE* locus of *B. subtilis*. Strains EK1 (a) and EK2 (b) were grown to log phase in *Bacillus* medium changing the concentration of exogenous guanine in a dose-response curve and assayed for reporter activity by Miller assay. (c and d) Strains EK1 (c) and EK2 (d) were grown to log phase in *Bacillus* medium or in the presence of 1 mM exogenous guanine, hypoxanthine, adenine, or xanthine and assayed for reporter activity by Miller assay. (e) *S. aureus xpt*-riboswitch reporter was integrated into the *rmpF-isdB* locus of *S. aureus* and grown to log phase in tryptic soy broth supplemented with 1 mM exogenous guanine, guanosine, hypoxanthine, xanthine, adenine, 2-aminopurine, 2′-deoxyguanosine, 6-thioguanine, and 2-acetamido-6-hydroxypurine, and reporter activity was measured. (f) Water-LOGSY NMR spectra of guanine (C and D) and adenine (A and B) in the presence (A and C) and absence (B and D) of purified riboswitch aptamer. The guanine signal at 7.95 ppm corresponds to the proton in position 8 of the purine ring. The change in sign upon the addition of riboswitch RNA to guanine indicates that the nucleotide is interacting (C and D). The adenine signals at 8.1 and 8.15 ppm correspond to the protons in position 2 and 8. There is no sign change upon the addition of riboswitch to adenine (A and B). The broad signals at 6.2 ppm (in guanine) and 6.8 ppm (in adenine) correspond to the NH_2 groups. These protons exchange with the bulk water, leading to a strong negative signal in all spectra that has no information for binding interaction. The signal at 0 ppm corresponds to the resonance of 2,2-dimethylsilapentane-5-sulfonic acid (DSS). Other signals visible in the riboswitch spectra stem from buffer impurities. Results are presented as means ± standard deviations (SD) (error bars) or means plus SD ($n = 3$) (a to e). Statistical analyses were performed using Student's *t* test. Values that are statistically significantly different from the value for the control (vehicle) are indicated by asterisks as follows: *, $P < 0.05$; **, $P < 0.01$; ***, $P < 0.001$.

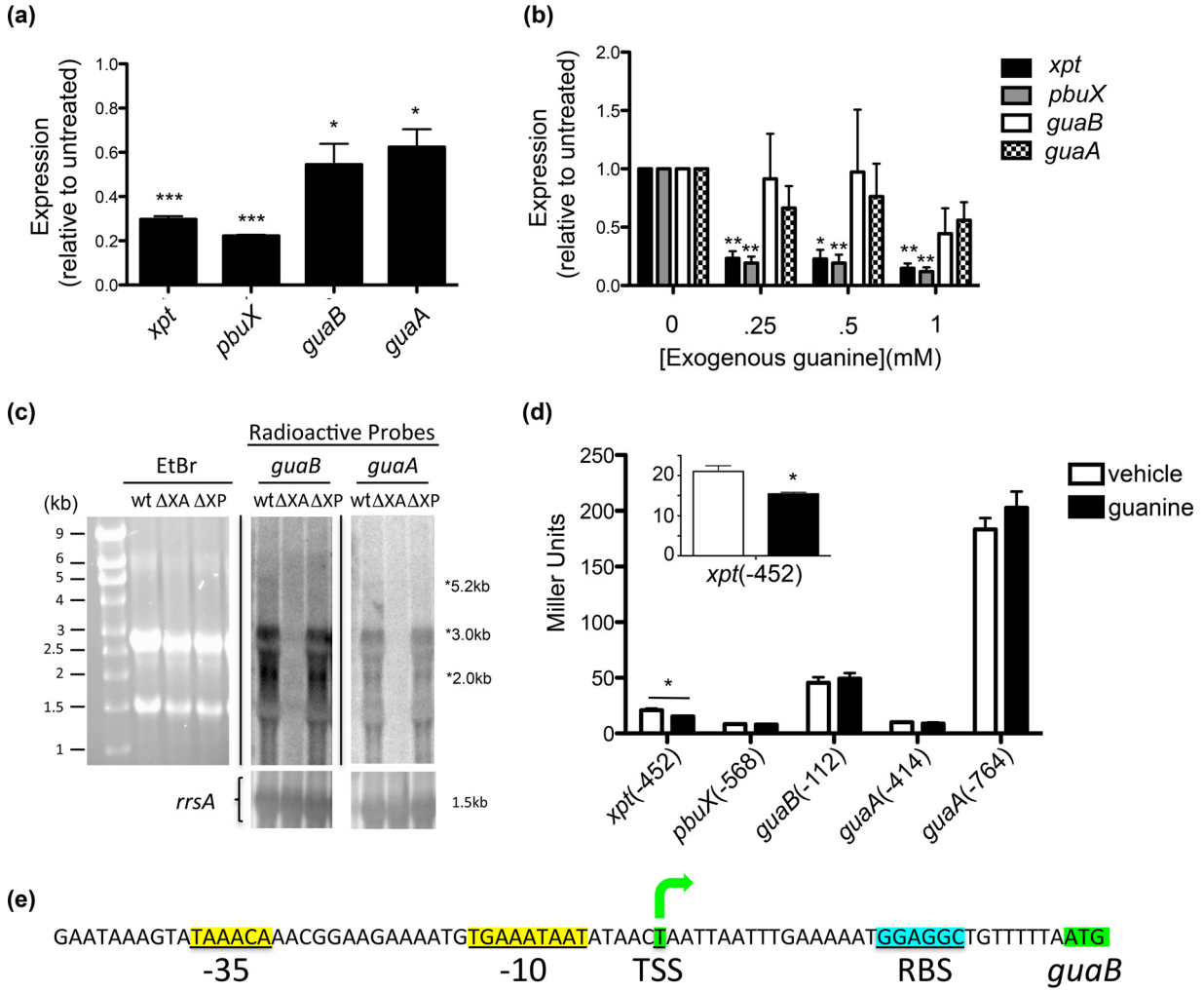

FIG 3 Guanine inhibits endogenous expression of *xpt-pbuX-guaB-guaA* and reveals the existence of alternative promoters for *guaB* and *guaA*. (a) *xpt*, *pbuX*, *guaB*, and *guaA* transcripts were quantified by TaqMan qRT-PCR on RNA collected from overnight cultures of *S. aureus* grown in chemically defined medium (CDM) lacking guanine with or without the addition of 1 mM exogenous guanine and are presented as expression relative to untreated *S. aureus* cultures using the $2^{-\Delta\Delta C_T}$ method (17). (b) Transcripts were quantified as in panel a from RNA derived from log-phase *S. aureus* cultures grown in tryptic soy broth supplemented with 0, 0.25, 0.5, and 1 mM guanine. qRT-PCR data (a and b) are means ± SD ($n = 3$), and each reaction was normalized to the rRNA *rrsA*. (c) Total RNA was isolated from wild-type (wt), Δ*xpt-guaA* (ΔXA), and Δ*xpt-pbuX* (ΔXP) *S. aureus* strains grown to log phase in TSB, separated by denaturing agarose gel electrophoresis, transferred to nylon membrane, and Northern blotted for *guaB* and *guaA* using [α-^{32}P]dCTP-labeled radioactive DNA probes, or stained with ethidium bromide (EtBr) to verify RNA integrity. The blots were subsequently probed for ribosomal 16S RNA *rrsA* as a loading control. (d) *S. aureus* with transcriptional *lacZ*-reporter constructs *xpt*(−452), *pbuX*(−568), *guaB*(−112), *guaA*(−414), and *guaA*(−764) were grown to log phase in CDM with or without 1 mM exogenous guanine, and reporter activity was measured using the Miller assay. Miller units are reported as means plus SD ($n = 3$). (e) 5′-RACE mapped the *guaB* transcriptional start site (TSS) (green) 31 bp upstream of the translational start codon, and the ribosomal binding site (cyan) and sigma factor-binding site (yellow) were predicted computationally (25). Statistical analyses were performed using Student's *t* test. Values that are significantly different are indicated by asterisks as follows: *, $P < 0.05$; **, $P < 0.01$; ***, $P < 0.001$.

We then sought to identify the transcriptional start site of the alternative promoter in front of the major *guaB-guaA* bicistronic operon by 5′-RACE PCR. This method identified a single transcriptional start site located 31 bases upstream of the *guaB* start codon (Fig. 3e; see Fig. S3 in the supplemental material). This promoter site is predicted computationally with high confidence by bacterial sigma70 promoter recognition software (25).

Contributions of purine salvage and *de novo* guanine biosynthesis on growth in defined medium and human serum. Nutritional requirements for the growth of *S. aureus* in human serum and during infection are largely unexplored, but evidence suggests that many bacterial pathogens absolutely require *de novo* nucleotide biosynthesis for virulence (26–34). To determine the importance of *de novo* guanine biosynthesis and purine salvage to the growth and virulence of *S. aureus*, we generated an unmarked clean deletion of *xpt-pbuX* (EK8; Δ*xpt-pbuX*), a strain in which *xpt-pbuX-guaB-guaA* genes were deleted (EK10; Δ*xpt-guaA*), introduced stop codons in *guaB* (EK11; *guaB*-KO [*guaB* knocked out]) or *guaA* (EK12; *guaA*-KO), and generated a strain *pbuX*::Tn (EK9), in which the *pbuX* locus containing a transposon insertion was transduced into strain NRS384 (Table 1).

Growth in tryptic soy broth (TSB) revealed a severe growth defect of Δ*xpt-guaA*, *guaB*-KO, and *guaA*-KO strains (Fig. 4a) characterized by an extended lag phase and achievement of about

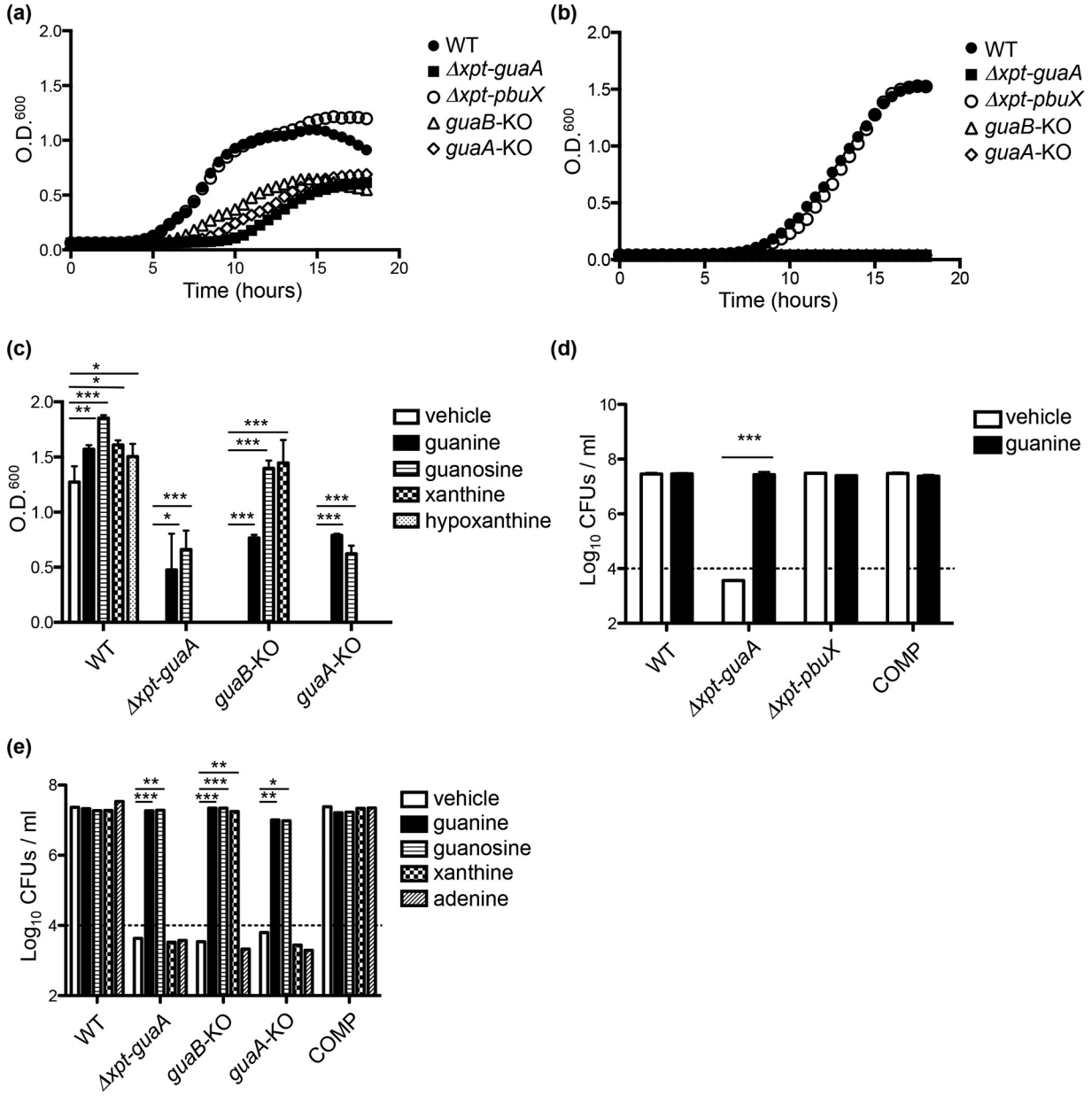

FIG 4 *De novo* guanine biosynthesis genes *guaB* and *guaA*, but not the purine salvage genes *xpt* and *pbuX*, are required for growth of *S. aureus* in defined medium lacking guanine and in human serum. (a and b) WT, Δ*xpt-guaA*, Δ*xpt-pbuX*, *guaB*-KO, and *guaA*-KO strains of *S. aureus* were grown to log phase in TSB, washed in PBS, and seeded at 5×10^4 CFU/ml in fresh TSB (a) or CDM (b) and monitored for growth by measuring optical density at 600 nm ($O.D.^{600}$) over 18 h. (c) Purine auxotrophy of WT, Δ*xpt-guaA*, *guaB*-KO, and *guaA*-KO strains of *S. aureus* was determined by measuring optical density at 600 nm after 15 h of growth in CDM alone (vehicle; 0.002 N NaOH) or supplemented with 1 mM guanine, guanosine, xanthine, or hypoxanthine. (d) Guanine auxotrophy of WT, Δ*xpt-guaA*, and Δ*guaB* strains and the isogenic complemented (COMP) strain were determined by growth in 100% human male A/B heat-inactivated serum (pH buffered with 5 mM HEPES) alone or supplemented with 1 mM guanine, and CFU were enumerated after 24 h. (e) Purine auxotrophy of WT, Δ*xpt-guaA*, *guaB*-KO, *guaA*-KO, and COMP strains in human serum were determined as described above for panel d. Growth kinetic experiments (a to c) were performed in 200-μl volumes in an incubated (37°C) plate reader, and CFU experiments (d and e) were performed in 3-ml shaking cultures at 37°C using an input of 1×10^4 CFU/ml (dashed line). Results are presented as the means of four replicate experiments (a and b) and means plus SD ($n = 3$) (c to e). Statistical analyses were performed using Student's *t* test. Values that are significantly different are indicated by bars and asterisks as follows: *, $P < 0.05$; **, $P < 0.01$; ***, $P < 0.001$.

half the cell density (in 96-well format) as that of the wild-type (WT) strain after 18 h, whereas no significant defects were observed in either the Δ*xpt-pbuX* (Fig. 4a) or *pbuX*::Tn strain (see Fig. S4a in the supplemental material). Growth in chemically defined medium lacking purines shows that Δ*xpt-guaA*, *guaB*-KO, and *guaA*-KO strains are guanine auxotrophs, whereas the purine salvage pathway mutants have no growth defect (Fig. 4b; see Fig. S4b). With the exception of guanine and guanosine, the other natural purines cannot reverse this defect, but xanthine does rescue growth of the *guaB*-KO strain, as expected from the order of steps in guanine biosynthesis (Fig. 4c and 1a). We suspect that guanine and guanosine are able to support growth of the knockout

strains because they are efficiently imported by a nucleobase transporter and can be converted into essential guanine derivatives (Fig. 1a) (35).

We then asked whether *de novo* purine biosynthesis is required for growth of *S. aureus* in human serum where the concentration of free guanine is not detected (36, 37) and may more accurately reflect *in vivo* conditions during an infection (26, 38). To test this, we compared growth of the guanine auxotroph Δ*xpt-guaA* to the guanine prototrophic WT, Δ*xpt-pbuX*, and isogenic complemented (COMP; EK14) strains in 100% heat-inactivated human serum. Interestingly, the Δ*xpt-guaA* strain completely failed to grow in human serum and actually lost CFU over time, whereas all of the prototrophic strains achieve 3 log units of growth in 24 h (Fig. 4d). As expected, the Δ*xpt-guaA* failure to proliferate is completely reversed by the addition of exogenous guanine. Functional *guaB* or *guaA* is individually essential for growth in human serum, as shown by the complete growth failure of *guaB*-KO and *guaA*-KO strains (Fig. 4e). Growth of the *guaB*-KO strain was rescued by the addition of exogenous xanthine, whereas growth of the *guaA*-KO strain was not rescued (Fig. 4e), as predicted by the sequence of the purine biosynthetic pathway in *S. aureus* (Fig. 1a) and as observed in Fig. 4c. As a control, supplementation of serum with adenine did not restore growth of any mutant strain (Fig. 4e). Together, these results indicate that human serum does not contain sufficient free nucleotides to support growth of *S. aureus* in the absence of the *de novo* guanine biosynthetic pathway.

Effects of *xpt*, *pbuX*, *guaB*, and *guaA* on virulence of *S. aureus in vivo*. To evaluate the requirement of the purine biosynthetic pathway during infection, we tested the WT, Δ*xpt-pbuX*, and *pbuX*::Tn strains for virulence in a mouse bacteremia model by intravenous injection of early log-phase bacteria (2×10^6 CFU/mouse) and enumerated bacteria from the kidneys at 1 and 3 days postinfection. Although the purine salvage pathway-defective Δ*xpt-pbuX* and *pbuX*::Tn mutants exhibited a marginal but significant reduction in kidney colonization on day 1, by day 3 they were not different from the wild-type (Fig. 5a) ($P = 0.84$ and $P = 0.69$, respectively). In contrast, the Δ*xpt-pbuX-guaB-guaA* strain had a 2-log-unit reduction in kidney colonization on day 1 (Fig. 5b) ($P = 0.0079$), and infection was completely cleared by all mice on day 3 (Fig. 5b) ($P = 0.0075$). The virulence of the complemented strain was identical to that of the WT on both day 1 (Fig. 5b) ($P = 1.0$) and day 3 (Fig. 5b) ($P = 1.0$), demonstrating that the phenotype observed in the knockout was specific to deletion of *xpt-pbuX-guaB-guaA* and not a result of an unidentified mutation. Like the Δ*xpt-pbuX-guaB-guaA* strain, the *guaB*-KO and *guaA*-KO strains were significantly reduced on day 1 (Fig. 5c) ($P = 0.0079$ and $P = 0.0117$, respectively), and completely cleared by day 3 (Fig. 5c) ($P = 0.0097$).

We then tested COMP, Δ*xpt-pbuX*, Δ*xpt-pbuX-guaB-guaA*, *guaB*-KO, and *guaA*-KO strains in the neutropenic thigh model of infection, where 2×10^5 bacteria were injected into one thigh muscle and CFU were enumerated 24 h later. In this model, the Δ*xpt-pbuX-guaB-guaA* ($P = 0.0079$), *guaB*-KO ($P = 0.0079$), and *guaA*-KO ($P = 0.0079$) strains were severely attenuated for virulence, whereas the Δ*xpt-pbuX* strain was not ($P = 0.0556$) (Fig. 5d). Treatment of COMP-infected mice with vancomycin ($P = 0.0079$) served as a control for inhibition of bacterial growth (Fig. 5d). Together, these data demonstrated that *guaB* and *guaA* were individually essential for virulence of *S. aureus in vivo*, whereas *xpt* and *pbuX* were dispensable. Interestingly, when we genotyped bacteria recovered from the kidneys of mice infected with *guaB*-KO and *guaA*-KO strains 24 h after infection (Fig. 5d), we identified the presence of stop codon revertants (Fig. 5d legend). This suggested that the log unit difference in bacterial growth observed between the Δ*xpt-pbuX-guaB-guaA* clean deletion and *guaB*-KO or *guaA*-KO was the result of selection for reversion to guanine prototrophy *in vivo*. Reversion was not observed in the clean deletion Δ*guaB* strain (Fig. 5e). Together, these data highlight the importance of *de novo* guanine biosynthesis in the growth and survival of *S. aureus* during infection due to limitation of free guanine *in vivo*.

***De novo* guanine biosynthesis is required for growth, survival, and maintenance of normal cell morphology of *S. aureus* in medium lacking guanine.** We then compared the growth phenotype of the Δ*guaB* strain (EK13) to that of the Δ*xpt-guaA* strain and found that growth of the Δ*guaB* strain in TSB was defective but not nearly as severe as that of the Δ*xpt-guaA* strain (Fig. 6a). We then tested whether growth of the Δ*guaB* strain was defective in defined medium lacking guanine and found that *guaB* deletion phenocopies the strict guanine auxotrophy observed for the Δ*xpt-guaA* strain (Fig. 6b). Strikingly, when we compared the growth and survival of the WT to the Δ*guaB* strain in shaking cultures, while there was no difference in recoverable CFU in rich broth (Fig. 6c), in CDM, loss of recoverable CFU was detected by day 2, and by day 6, no CFU could be recovered (Fig. 6d). When both WT and Δ*guaB* strains were grown in rich broth (TSB), there were no obvious differences between the strains in external matrix thickness and septation (Fig. 6e; see Fig. S5 in the supplemental material). At day 3 after transfer to medium lacking guanine, the Δ*guaB* cells displayed marked phenotypic abnormalities (Fig. 6e; see Fig. S5). The most striking difference was a pronounced lamellated thickening of the external matrix from ~30 nm in input (both WT and Δ*guaB* strains) to ~150 nm in the Δ*guaB* strain on day 3 (Fig. 6e and f; see Fig. S5). This defect occurred in 95% of the Δ*guaB* cells at day 3 and in none of the WT cells. A second defect seen in day 3 Δ*guaB* cells was abnormal division septa (Fig. 6e and g; see Fig. S5). In day 3 Δ*guaB* cells, we observed few (5%) morphologically normal trilamellar planes of cell division, whereas ~50% of WT cell profiles at day 3 and ~50% of the input WT and input Δ*guaB* cell profiles had morphologically normal division septae (Fig. 6g). Instead, division septae in day 3 Δ*guaB* cells, which were present at a frequency comparable to that of WT cells, were markedly thickened and only rarely trilaminar.

Bactericidal analog PC1 mode of action is independent of the guanine riboswitch. The development of riboswitch-binding nucleotide analogs suggested that inhibition of expression of essential genes regulated by these gene regulatory elements may be possible (39). Based on the crystal structure of hypoxanthine bound to a guanine riboswitch (22), it was proposed that purine and pyrimidine analogs could also form a network of hydrogen bonds for proper complex formation between ligand and aptamer (7). A pyrimidine analog 2,5,6-triaminopyrimidin-4-one (PC1) was reported to kill *S. aureus* but not bacteria that lack guanine riboswitch control of *guaA* (7, 8). We tested the antibiotic potential of PC1 against *S. aureus*, *Staphylococcus epidermidis*, *Bacillus subtilis*, *Klebsiella pneumoniae*, *Enterococcus faecalis*, and *Escherichia coli* and confirmed that PC1 indeed kills *Staphylococcus* but not the other Gram-positive and -negative bacteria examined (see Fig. S6 in the supplemental material).

Since our data suggested that there were riboswitch-indepen-

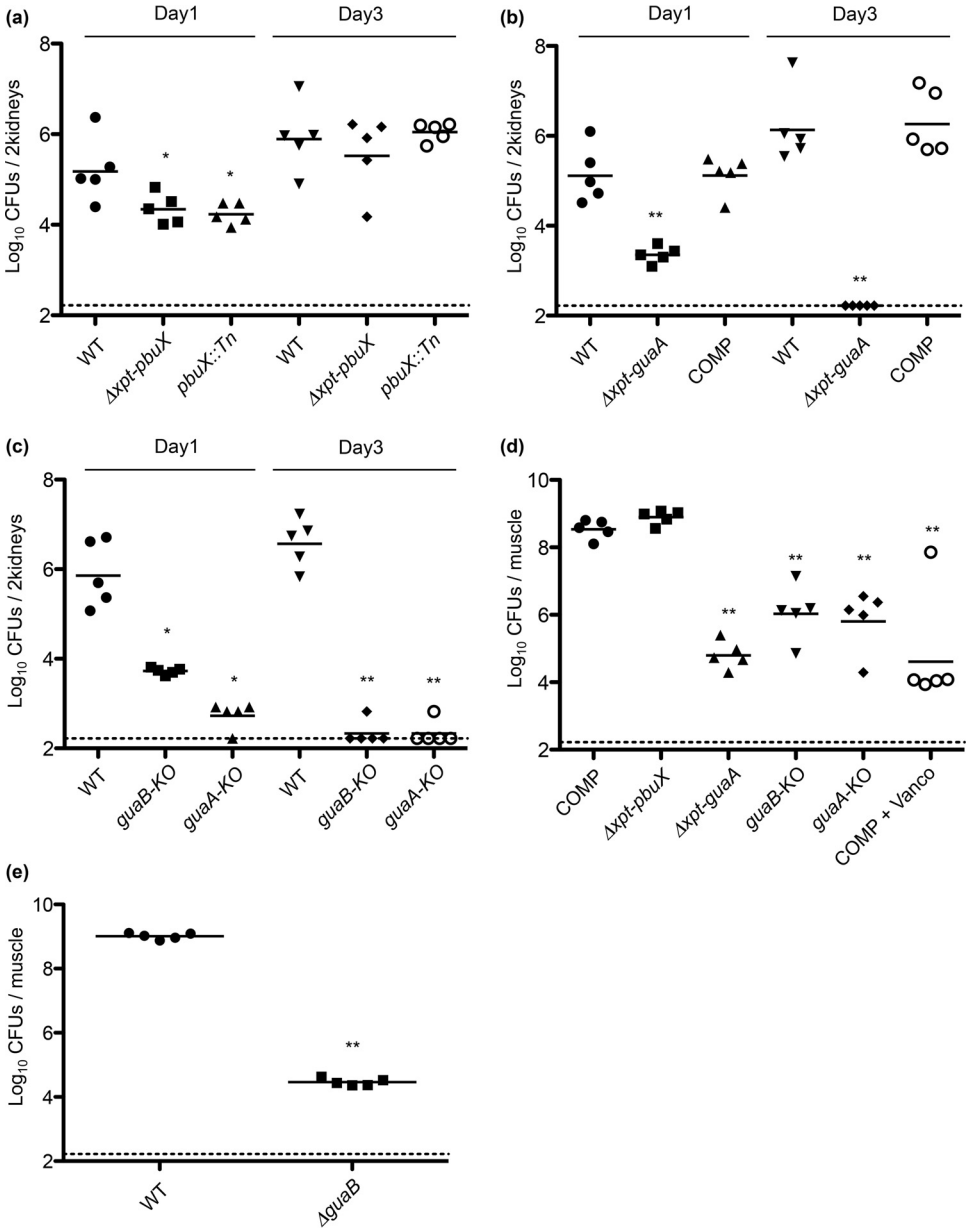

FIG 5 *guaB* and *guaA* are required for virulence of *S. aureus in vivo*. (a) WT, Δ*xpt-pbuX*, and *pbuX*::Tn strains were evaluated for virulence in the murine A/J intravenous bacteremia model of infection by injection of 2×10^6 CFU per mouse, and the kidneys were harvested for enumeration of CFU 1 and 3 days postinfection. Significant differences between the values for the WT strain and Δ*xpt-pbuX* strain ($P = 0.0317$ [*]) and *pbuX*::Tn strain ($P = 0.0362$ [*]) were observed on day 1, but no significant difference was observed on day 3 (WT and Δ*xpt-pbuX* strains, $P = 0.8413$; WT and *pbuX*::Tn strains, $P = 0.6905$). (b) WT, Δ*xpt-guaA*, and COMP strains were evaluated for virulence in the murine A/J intravenous bacteremia model of infection as in panel a. Significant differences between WT and Δ*xpt-guaA* strains ($P = 0.0079$ [**]) but not between WT and COMP strains ($P = 1.0$) were observed on day 1 and on day 3 (WT and Δ*xpt-guaA* strains, $P = 0.0075$ [**]; WT and COMP strains, $P = 1.0$). (c) The individual contribution of *guaB* and *guaA* genes to virulence was determined by infection of mice with WT, *guaB*-KO, and *guaA*-KO strains followed by enumeration of kidney CFU on day 1 and day 3 postinfection. Significant differences were observed on day 1 between the WT strain and *guaB*-KO strain ($P = 0.0079$ [**]) and *guaA*-KO strain ($P = 0.0117$ [*]) and on day 3 (WT and *guaB*-KO strains, $P = 0.0097$ [**]; WT and *guaA*-KO strains, $P = 0.0097$ [**]). (d) Virulence of COMP, Δ*xpt-pbuX*, Δ*xpt-guaA*, *guaB*-KO, and *guaA*-KO strains were determined in a neutropenic thigh model of infection where neutrophils in CD1 mice are depleted by cyclophosphamide injection, followed by infection of 2×10^5 CFU/thigh muscle, and enumeration of CFU 24 h later. There was no difference between the COMP and Δ*xpt-pbuX* strains ($P = 0.0556$), but marked differences between the COMP strain and the Δ*xpt-guaA* strain ($P = 0.0079$ [**]), *guaB*-KO strain ($P = 0.0079$ [**]), and *guaA*-KO strain ($P = 0.0079$ [**]). Mice infected with the COMP strain and then injected intraperitoneally with vancomycin (Vanco) were used as a control ($P = 0.0079$ [**]). Bacteria recovered from the *guaB*-KO and *guaA*-KO infected mice were genotyped for *guaB* and *guaA*, respectively, and revealed outgrowth of stop codon revertants in 4/5 mice with the exception of the individual with the lowest CFU recovered. (e) Virulence of the Δ*guaB* strain was determined in the neutropenic thigh model described above for panel d and was significantly different from the WT strain ($P = 0.0079$ [**]). All *in vivo* experiments were performed on groups of five mice, and statistical significance was determined by Mann-Whitney test. Each graph represents data from a single experiment. Each symbol represents the value for an individual mouse, and each bar shows the mean for that group of mice. The limit of detection was 166 CFU/ml as indicated by the dashed line. All experiments were performed at least three times with similar results.

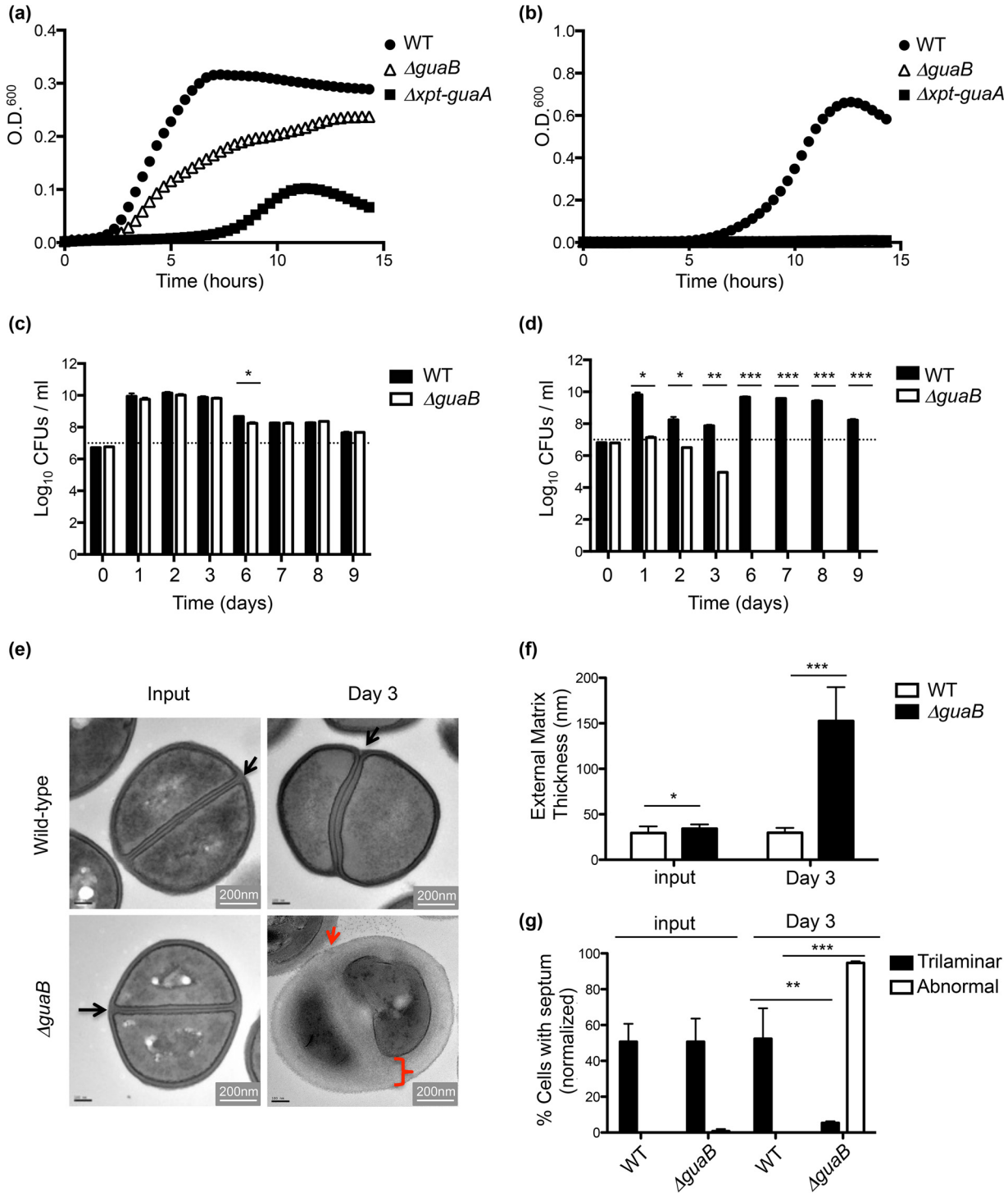

FIG 6 *De novo* guanine biosynthesis is essential for growth, survival, and maintenance of normal cell morphology of *S. aureus* in medium lacking guanine. (a) WT, Δ*guaB*, and Δ*xpt-guaA* strains of *S. aureus* were grown to log phase in TSB, washed with PBS, seeded at 1×10^5 CFU/ml in fresh TSB, and monitored for growth by measuring optical density at 600 nm for 14 h. (b) Growth of WT, Δ*guaB*, and Δ*xpt-guaA* strains of *S. aureus* was measured as described above for panel a but using CDM. (c) Survival of WT and Δ*guaB* strains grown in TSB in 100-ml shaking cultures at 37°C was monitored over time by enumeration of CFU (input of 1×10^7 CFU/ml indicated by the dashed line). (d) Survival of WT and Δ*guaB* strains grown in CDM was monitored over time as described for panel c. (e) Transmission electron microscopy was performed on WT and Δ*guaB* cells processed from input and 3 days after shift from TSB into CDM lacking guanine. Black arrows highlight the normal trilamellar division septum in WT cells (input and day 3) and Δ*guaB* cells (input only). The red arrow highlights a dysmorphic division septum in day 3 Δ*guaB* cells. (f) External matrix thickness was measured from images collected at a magnification of ×40,000 for WT input (29.4 ± 7.3 nm; $n = 12$), Δ*guaB* input (34.2 ± 4.7 nm; $n = 22$), WT day 3 (29.7 ± 5.4 nm; $n = 14$), and Δ*guaB* day 3 (152.6 ± 37.1 nm; $n = 26$). Significant differences in thickness were observed between WT and Δ*guaB* input ($P = 0.027$ [*]) and WT and Δ*guaB* day 3 ($P < 0.0001$ [***]). (g) Cells from three random TEM fields imaged at ×2,000 were scored for the presence of division structures, normal trilaminar division septa, and abnormal septa from WT input ($n = 90$), Δ*guaB*

dent promoters for the essential *guaA* and *guaB* genes, we cultured WT *S. aureus* with 1 mM PC1 overnight in tryptic soy broth with or without 1 mM exogenous guanine. Although 1 mM guanine should recover bacterial growth in the absence of *guaA* and *guaB* (Fig. 4), we obtained no recoverable CFU in the presence of PC1, whether or not guanine was present (see Fig. S6b in the supplemental material). Supplementation of Mueller-Hinton broth with GMP, AMP, and guanine all failed to rescue *S. aureus* from the cytotoxic effects of PC1 (see Fig. S7). Importantly, failure of guanine to rescue cell viability demonstrated that the antibiotic activity of PC1 cannot result solely from inhibition of guanine biosynthesis. To determine whether endogenous *xpt*, *pbuX*, *guaB*, and *guaA* transcripts were affected by PC1, we performed qRT-PCR on RNA collected from log-phase *S. aureus* grown in tryptic soy broth in the presence of various amounts of PC1. Surprisingly, repression of endogenous gene expression was not observed for *xpt*, *pbuX*, *guaB*, nor *guaA* at any concentration (see Fig. S6c). We then tested whether PC1 influences reporter gene expression in *B. subtilis* carrying the *B. subtilis xpt* or *S. aureus xpt* reporter and found that PC1 did not alter reporter activity in either strain (see Fig. S6d). PC1 also failed to have any effect on the *S. aureus xpt* reporter stably integrated in *S. aureus* (see Fig. S6e).

Finally, to determine the whether PC1 toxicity required repression of the *xpt-pbuX-guaB-guaA* operon, we monitored the effects of 0.5 and 1 mM PC1 on the growth of WT and Δ*xpt-guaA* strains in Mueller-Hinton broth (see Fig. S6f in the supplemental material). The susceptibility of the Δ*xpt-guaA* strain to PC1 was indistinguishable from that of the WT, demonstrating that the bactericidal mode of action of PC1 is independent of the *xpt-pbuX-guaB-guaA* gene locus in *S. aureus*. Interestingly, PC1 was also cytotoxic to murine BALB/c peritoneal macrophages at the same concentration that it has activity against *S. aureus* despite the absence of purine riboswitches in mammalian cells (see Fig. S8). The identity and purity of PC1 were verified by analytical liquid chromatography-mass spectrometry (see Fig. S9).

The *nrdIEF* operon of *S. aureus* does not contain a guanine riboswitch in its 5′-UTR. Bioinformatic analysis of *S. aureus* N315 for noncoding regulatory elements had predicted that a purine riboswitch was located in the 5′-UTR of the nucleotide reductase *nrdI-nrdE-nrdF* operon (12). Because the *nrdI-nrdE-nrdF* operon appeared to be essential in both *B. subtilis* and *S. aureus* from an absence of insertions from transposon libraries (40) (41) and an inability to generate targeted disruptions in the operon (13), we tested whether this region encodes a bona fide guanine riboswitch.

To determine the level of similarity between *xpt* and *nrd* 5′-leader sequences, we generated pairwise sequence alignments of the *S. aureus nrd* 5′-UTR and the *S. aureus xpt* 5′-UTR (see Fig. S10a in the supplemental material). There was considerable deviation from nucleotides conserved in guanine-binding riboswitch aptamers, and the predicted secondary structure of the *nrd* leader region fails to form the typical three-junction stem-loop structure (see Fig. S10b). These observations argue against a guanine-responsive riboswitch at the *nrd* promoter. To test this hypothesis experimentally, we performed qRT-PCR on RNA from *S. aureus* grown in CDM overnight in the presence or absence of 1 mM guanine and measured transcript abundance of *nrdI*, *nrdE*, and *nrdF* relative to the untreated controls. Exogenous guanine had no significant effect on transcript abundance of *nrdI*, *nrdE*, nor *nrdF* (see Fig. S10c), suggesting the absence of a guanine-responsive riboswitch in this promoter. In an additional experiment, we isolated RNA from log-phase cultures of *S. aureus* grown in TSB with various concentrations of exogenous guanine but found no evidence that guanine significantly affects expression of *nrdI*, *nrdE*, and *nrdF* (see Fig. S10d). Finally, we generated an *S. aureus nrd* transcriptional reporter strain by fusion of the *nrd* promoter(−218 from transcriptional start site) (42) to *lacZ* stably integrated in *B. subtilis* [*nrd*(−218) (EK16)] (see Fig. S10e), and *S. aureus* [*nrd*(−218) (EK15)] (see Fig. S10f). Reporter activity was mildly but significantly repressed by guanine and significantly increased by adenine in *B. subtilis* (see Fig. S10e). Treatment with hydroxyurea stimulates expression from this promoter (13, 43), and we observed an ~16-fold induction of expression upon treatment (see Fig. S10e). In hydroxyurea-treated bacteria, there was a mild but significant reduction in reporter activity upon guanine treatment. In contrast, reporter activity in *S. aureus* was very low and not significantly altered by culture with guanine or adenine (see Fig. S10f). The *S. aureus nrd* promoter was not strongly active in a variety of culture conditions tested, including anaerobic growth, log, nor in stationary phase (data not shown). In total, the data suggest that the *nrd* 5′-UTR of *S. aureus* does not contain a guanine riboswitch.

DISCUSSION

Here we demonstrate both in mouse infection models and in human serum, that guanine limitation constrains virulence of *S. aureus* and that the purine salvage pathway was dispensable. Although we ruled out the guanine riboswitch as a potential antibiotic target in *S. aureus*, this study provides several new insights into the regulation of the *xpt*, *pbuX*, *guaB*, and *guaA* genetic locus. We confirm the existence of a bona fide guanine riboswitch in the *S. aureus xpt*-5′-UTR that tightly regulated the expression of the purine salvage pathway enzymes *xpt* and *pbuX*. However, the proposed four-gene operon can be separated into at least three independent transcriptional units, the major species being a 3.0-kb bicistronic *guaB-guaA* operon and alternative 2-kb *guaA* transcript, and a minor 5.2-kb polycistronic *xpt-pbuX-guaB-guaA* four-gene operon. Most importantly, *guaB* and *guaA* were each individually essential for virulence and growth of *S. aureus in vivo*, and therefore constitute two potential antibiotic targets. Finally, the loss of *guaB* is bactericidal under conditions where guanine is limiting and is associated with profound morphological abnormalities in cell morphology. *De novo* guanine biosynthesis has been shown to be important for virulence of many bacterial

input ($n = 128$), WT day 3 ($n = 85$), and Δ*guaB* day 3 ($n = 73$). No differences in the frequency of normal trilaminar septum formation were observed for input (50.6% ± 10.7% for WT and 52.3% ± 16.9% for Δ*guaB* strain; $P = 0.889$), but on day 3 few trilaminar septa were observed in the Δ*guaB* strain (5.3% ± 0.9%) compared to the WT (50.6% ± 12.9%) ($P = 0.0038$ [**]). On day 3, 94.7% ± 0.85% of Δ*guaB* cells containing division structures were abnormal. The frequency of normal trilaminar or abnormal septum was calculated by normalization to the total number of cells with visible division structures in each field ($n = 3$). Growth kinetic experiments (a and b) were performed in 100-μl volumes in an incubated (37°C) plate reader. Results are presented as the means of 16 replicates (a and b) and means plus SD ($n = 3$) (c and d). Statistical analyses were performed using Student's *t* test. Values that are significantly different are indicated by bars and asterisks as follows: *, $P < 0.05$; **, $P < 0.01$; ***, $P < 0.001$.

pathogens (26–34) but has never been demonstrated for *S. aureus*. The data presented here show that the purine salvage pathway appears to be much less important than the *de novo* synthesis pathway during infection.

We are currently striving to identify the composition of the thickened external matrix in the Δ*guaB* cells as observed in the electron microscopy images and to understand why cell viability deteriorates in this strain. Previous work has shown that pharmacological inhibition of *guaA* in *B. subtilis* prevents peptidoglycan turnover and recycling (44), but the cause of this phenotype was never mechanistically explained. Cell wall thickening by ~10 nm has been linked to vancomycin resistance in *S. aureus* and was characterized by TEM (45), but the morphology of those strains bear no resemblance to the severe morphological defects we observe. Instead, the morphology more closely resembled *S. aureus* treatment with chloramphenicol (46). Whatever the molecular mechanism, bacteria lacking *guaB* clearly have severe problems with cell division that results in loss of viability.

The vast majority of *Firmicutes* maintain *xpt* under direct riboswitch regulation typically in a two-gene operon with *pbuX* (47), but maintain *guaB* and *guaA* as separate genes, of which only a small subset are reported to be directly regulated by a purine riboswitch (47). In retrospect, the existence of complex regulation of *guaB* and *guaA* expression is not surprising, given the critical role that *de novo* guanine biosynthesis plays in bacterial growth and virulence.

Because the guanine riboswitch was reported to regulate the *de novo* synthesis pathway in *S. aureus*, we evaluated the feasibility of developing small-molecule drugs that bind the bacterial guanine riboswitch and prevent the expression of genes essential for the survival and virulence of *S. aureus*. Here we provide several lines of evidence to suggest that this approach will not be useful to treat *S. aureus* infection. First, the *xpt*-riboswitch exclusively regulated only the transcription of *xpt* and *pbuX*, and the Δ*xpt-pbuX* strain was not defective in virulence in two murine infection models (Fig. 5a and d). Second, the guanine analog 2-acetamido-6-hydroxypurine strongly repressed riboswitch reporter activity but failed to alter growth in chemically defined and rich media (Fig. 2g; see Fig. S1 in the supplemental material). Third, individually, *guaB* and *guaA* were essential for virulence *in vivo* but were regulated by alternative promoters independent from control by the guanine riboswitch. Fourth, we found no evidence that the *nrdIEF* operon was controlled by a guanine riboswitch in *S. aureus*, suggesting that no essential genes were strictly controlled by a guanine riboswitch in *S. aureus* (see Fig. S10). Finally, the antibiotic activity of PC1, which was reported to have selectivity for the guanine riboswitch, appeared to result from effects independent of this target (see Fig. S6 to S8).

Similar to PC1, the antibiotic lysine analog *S*-(2-aminoethyl)-L-cysteine (AEC) binds the lysine riboswitch (9, 48, 49) but has also been clearly demonstrated to have other cellular targets (50), including being directly incorporated into proteins (51, 52). Surprisingly, high-affinity riboswitch ligand analogs do not always modulate transcription (3, 53, 54), which adds another layer of complexity to an already daunting challenge of developing antibiotics that target the riboswitch. However, two recent reports have identified small-molecule inhibitors targeting the riboflavin riboswitch that have *in vivo* activity against *E. coli* (55) and *C. difficile* (60).

Despite the shortfalls of the guanine riboswitch as an antibiotic target in *S. aureus*, it remains possible that *guaB* or *guaA* is regulated by this mechanism in other bacterial pathogens. The inability of *guaB* and *guaA* mutants to survive *in vivo*, in medium lacking guanine, and in human serum indicates that guanine is severely limiting and suggests that targeting these proteins may have therapeutic value for persistent bacterial infections.

ACKNOWLEDGMENTS

E.M.K. and M.-W.T designed all experiments, and E.M.K. executed all experiments and performed all data analysis with the following exceptions: C.D.A., M.R., and A.K.K. designed and executed transmission electron microscopy experiments; M.X., D.Y., J.K., and S.P. performed all *in vivo* infections and organ harvest; T.M. designed and performed water-LOGSY NMR of RNA aptamers; B.L. performed LC/MS analysis of purchased compounds to verify identity and purity; S.V.D. performed computational analysis of the USA300 (NRS384) genome; and I.R.M. constructed pIMC85.

FUNDING INFORMATION

This work, including the efforts of Eric Matthew Kofoed, Donghong Yan, Anand K. Katakam, Mike Reichelt, Baiwei Lin, Janice Kim, Summer Park, Shailesh V. Date, Min Xu, Cary D. Austin, Till Maurer, and Man-Wah Tan, was funded by Genentech (Genentech, Inc.).

REFERENCES

1. **Roth A, Breaker RR.** 2009. The structural and functional diversity of metabolite-binding riboswitches. Annu Rev Biochem **78:**305–334. http://dx.doi.org/10.1146/annurev.biochem.78.070507.135656.
2. **Serganov A, Nudler E.** 2013. A decade of riboswitches. Cell **152:**17–24. http://dx.doi.org/10.1016/j.cell.2012.12.024.
3. **Kim JN, Blount KF, Puskarz I, Lim J, Link KH, Breaker RR.** 2009. Design and antimicrobial action of purine analogues that bind guanine riboswitches. ACS Chem Biol **4:**915–927. http://dx.doi.org/10.1021/cb900146k.
4. **Mandal M, Boese B, Barrick JE, Winkler WC, Breaker RR.** 2003. Riboswitches control fundamental biochemical pathways in Bacillus subtilis and other bacteria. Cell **113:**577–586. http://dx.doi.org/10.1016/S0092-8674(03)00391-X.
5. **Brinsmade SR, Sonenshein AL.** 2011. Dissecting complex metabolic integration provides direct genetic evidence for CodY activation by guanine nucleotides. J Bacteriol **193:**5637–5648. http://dx.doi.org/10.1128/JB.05510-11.
6. **Cho BK, Federowicz SA, Embree M, Park YS, Kim D, Palsson BO.** 2011. The PurR regulon in Escherichia coli K-12 MG1655. Nucleic Acids Res **39:**6456–6464. http://dx.doi.org/10.1093/nar/gkr307.
7. **Mulhbacher J, Brouillette E, Allard M, Fortier LC, Malouin F, Lafontaine DA.** 2010. Novel riboswitch ligand analogs as selective inhibitors of guanine-related metabolic pathways. PLoS Pathog **6:**e1000865. http://dx.doi.org/10.1371/journal.ppat.1000865.
8. **Ster C, Allard M, Boulanger S, Lamontagne Boulet M, Mulhbacher J, Lafontaine DA, Marsault E, Lacasse P, Malouin F.** 2013. Experimental treatment of Staphylococcus aureus bovine intramammary infection using a guanine riboswitch ligand analog. J Dairy Sci **96:**1000–1008. http://dx.doi.org/10.3168/jds.2012-5890.
9. **Blount KF, Wang JX, Lim J, Sudarsan N, Breaker RR.** 2007. Antibacterial lysine analogs that target lysine riboswitches. Nat Chem Biol **3:**44–49. http://dx.doi.org/10.1038/nchembio842.
10. **Daldrop P, Reyes FE, Robinson DA, Hammond CM, Lilley DM, Batey RT, Brenk R.** 2011. Novel ligands for a purine riboswitch discovered by RNA-ligand docking. Chem Biol **18:**324–335. http://dx.doi.org/10.1016/j.chembiol.2010.12.020.
11. **Lee ER, Blount KF, Breaker RR.** 2009. Roseoflavin is a natural antibacterial compound that binds to FMN riboswitches and regulates gene expression. RNA Biol **6:**187–194. http://dx.doi.org/10.4161/rna.6.2.7727.
12. **Geissmann T, Chevalier C, Cros MJ, Boisset S, Fechter P, Noirot C, Schrenzel J, Francois P, Vandenesch F, Gaspin C, Romby P.** 2009. A search for small noncoding RNAs in Staphylococcus aureus reveals a conserved sequence motif for regulation. Nucleic Acids Res **37:**7239–7257. http://dx.doi.org/10.1093/nar/gkp668.

13. **Masalha M, Borovok I, Schreiber R, Aharonowitz Y, Cohen G.** 2001. Analysis of transcription of the Staphylococcus aureus aerobic class Ib and anaerobic class III ribonucleotide reductase genes in response to oxygen. J Bacteriol **183:**7260–7272. http://dx.doi.org/10.1128/JB.183.24.7260-7272.2001.
14. **Monk IR, Shah IM, Xu M, Tan MW, Foster TJ.** 2012. Transforming the untransformable: application of direct transformation to manipulate genetically Staphylococcus aureus and Staphylococcus epidermidis. mBio **3:**e00277–11. http://dx.doi.org/10.1128/mBio.00277-11.
15. **Miller JH.** 1972. Experiments in molecular genetics. Cold Spring Harbor Laboratory Press, Cold Spring Harbor, NY.
16. **Zhang G, Mills DA, Block DE.** 2009. Development of chemically defined media supporting high-cell-density growth of lactococci, enterococci, and streptococci. Appl Environ Microbiol **75:**1080–1087. http://dx.doi.org/10.1128/AEM.01416-08.
17. **Pfaffl MW.** 2001. A new mathematical model for relative quantification in real-time RT-PCR. Nucleic Acids Res **29:**e45. http://dx.doi.org/10.1093/nar/29.9.e45.
18. **Livak KJ, Schmittgen TD.** 2001. Analysis of relative gene expression data using real-time quantitative PCR and the $2^{-\Delta\Delta CT}$ method. Methods **25:**402–408. http://dx.doi.org/10.1006/meth.2001.1262.
19. **Sambrook J, Fritsch EF, Maniatis T.** 1989. Molecular cloning: a laboratory manual, 2nd ed. Cold Spring Harbor Laboratory Press, Cold Spring Harbor, NY.
20. **Dalvit C, Pevarello P, Tato M, Veronesi M, Vulpetti A, Sundstrom M.** 2000. Identification of compounds with binding affinity to proteins via magnetization transfer from bulk water. J Biomol NMR **18:**65–68. http://dx.doi.org/10.1023/A:1008354229396.
21. **Mayer M, Meyer B.** 1999. Characterization of ligand binding by saturation transfer difference NMR spectroscopy. Angew Chem Int Ed **38:**1784–1788. http://dx.doi.org/10.1002/(SICI)1521-3773(19990614)38:12<1784::AID-ANIE1784>3.0.CO;2-Q.
22. **Batey RT, Gilbert SD, Montange RK.** 2004. Structure of a natural guanine-responsive riboswitch complexed with the metabolite hypoxanthine. Nature **432:**411–415. http://dx.doi.org/10.1038/nature03037.
23. **Gilbert SD, Mediatore SJ, Batey RT.** 2006. Modified pyrimidines specifically bind the purine riboswitch. J Am Chem Soc **128:**14214–14215. http://dx.doi.org/10.1021/ja063645t.
24. **Belitsky BR, Sonenshein AL.** 2013. Genome-wide identification of Bacillus subtilis CodY-binding sites at single-nucleotide resolution. Proc Natl Acad Sci U S A **110:**7026–7031. http://dx.doi.org/10.1073/pnas.1300428110.
25. **Solovyev V, Salamov A.** 2011. Automatic annotation of microbial genomes and metagenomic sequences, p 61–78. *In* Li RW (ed), Metagenomics and its applications in agriculture, biomedicine and environmental studies. Nova Science Publishers, Hauppauge, NY.
26. **Samant S, Lee H, Ghassemi M, Chen J, Cook JL, Mankin AS, Neyfakh AA.** 2008. Nucleotide biosynthesis is critical for growth of bacteria in human blood. PLoS Pathog **4:**e37. http://dx.doi.org/10.1371/journal.ppat.0040037.
27. **McFarland WC, Stocker BA.** 1987. Effect of different purine auxotrophic mutations on mouse-virulence of a Vi-positive strain of Salmonella dublin and of two strains of Salmonella typhimurium. Microb Pathog **3:**129–141. http://dx.doi.org/10.1016/0882-4010(87)90071-4.
28. **Santiago AE, Cole LE, Franco A, Vogel SN, Levine MM, Barry EM.** 2009. Characterization of rationally attenuated Francisella tularensis vaccine strains that harbor deletions in the guaA and guaB genes. Vaccine **27:**2426–2436. http://dx.doi.org/10.1016/j.vaccine.2009.02.073.
29. **Subashchandrabose S, Smith SN, Spurbeck RR, Kole MM, Mobley HL.** 2013. Genome-wide detection of fitness genes in uropathogenic Escherichia coli during systemic infection. PLoS Pathog **9:**e1003788. http://dx.doi.org/10.1371/journal.ppat.1003788.
30. **Le Breton Y, Mistry P, Valdes KM, Quigley J, Kumar N, Tettelin H, McIver KS.** 2013. Genome-wide identification of genes required for fitness of group A Streptococcus in human blood. Infect Immun **81:**862–875. http://dx.doi.org/10.1128/IAI.00837-12.
31. **Russo TA, Jodush ST, Brown JJ, Johnson JR.** 1996. Identification of two previously unrecognized genes (guaA and argC) important for uropathogenesis. Mol Microbiol **22:**217–229. http://dx.doi.org/10.1046/j.1365-2958.1996.00096.x.
32. **Morrow CA, Valkov E, Stamp A, Chow EW, Lee IR, Wronski A, Williams SJ, Hill JM, Djordjevic JT, Kappler U, Kobe B, Fraser JA.** 2012. De novo GTP biosynthesis is critical for virulence of the fungal pathogen Cryptococcus neoformans. PLoS Pathog **8:**e1002957. http://dx.doi.org/10.1371/journal.ppat.1002957.
33. **Noriega FR, Losonsky G, Lauderbaugh C, Liao FM, Wang JY, Levine MM.** 1996. Engineered deltaguaB-A deltavirG Shigella flexneri 2a strain CVD 1205: construction, safety, immunogenicity, and potential efficacy as a mucosal vaccine. Infect Immun **64:**3055–3061.
34. **Jewett MW, Lawrence KA, Bestor A, Byram R, Gherardini F, Rosa PA.** 2009. GuaA and GuaB are essential for Borrelia burgdorferi survival in the tick-mouse infection cycle. J Bacteriol **191:**6231–6241. http://dx.doi.org/10.1128/JB.00450-09.
35. **Jensen KF, Dandanell G, Hove-Jensen B, Willemoes M.** 18 August 2008, posting date. Nucleotides, nucleosides, and nucleobases. EcoSal Plus **2013** http://dx.doi.org/10.1128/ecosalplus.3.6.2.
36. **Eells JT, Spector R.** 1983. Purine and pyrimidine base and nucleoside concentrations in human cerebrospinal fluid and plasma. Neurochem Res **8:**1451–1457. http://dx.doi.org/10.1007/BF00965000.
37. **Liu Z, Li T, Wang E.** 1995. Simultaneous determination of guanine, uric acid, hypoxanthine and xanthine in human plasma by reversed-phase high-performance liquid chromatography with amperometric detection. Analyst **120:**2181–2184. http://dx.doi.org/10.1039/an9952002181.
38. **Traut TW.** 1994. Physiological concentrations of purines and pyrimidines. Mol Cell Biochem **140:**1–22. http://dx.doi.org/10.1007/BF00928361.
39. **Blount KF, Breaker RR.** 2006. Riboswitches as antibacterial drug targets. Nat Biotechnol **24:**1558–1564. http://dx.doi.org/10.1038/nbt1268.
40. **Kobayashi K, Ehrlich SD, Albertini A, Amati G, Andersen KK, Arnaud M, Asai K, Ashikaga S, Aymerich S, Bessieres P, Boland F, Brignell SC, Bron S, Bunai K, Chapuis J, Christiansen LC, Danchin A, Debarbouille M, Dervyn E, Deuerling E, Devine K, Devine SK, Dreesen O, Errington J, Fillinger S, Foster SJ, Fujita Y, Galizzi A, Gardan R, Eschevins C, Fukushima T, Haga K, Harwood CR, Hecker M, Hosoya D, Hullo MF, Kakeshita H, Karamata D, Kasahara Y, Kawamura F, Koga K, Koski P, Kuwana R, Imamura D, Ishimaru M, Ishikawa S, Ishio I, Le Coq D, Masson A, Mauel C, et al.** 2003. Essential Bacillus subtilis genes. Proc Natl Acad Sci U S A **100:**4678–4683. http://dx.doi.org/10.1073/pnas.0730515100.
41. **Fey PD, Endres JL, Yajjala VK, Widhelm TJ, Boissy RJ, Bose JL, Bayles KW.** 2013. A genetic resource for rapid and comprehensive phenotype screening of nonessential Staphylococcus aureus genes. mBio **4:**e00537–12. http://dx.doi.org/10.1128/mBio.00537-12.
42. **Hartig E, Hartmann A, Schatzle M, Albertini AM, Jahn D.** 2006. The Bacillus subtilis nrdEF genes, encoding a class Ib ribonucleotide reductase, are essential for aerobic and anaerobic growth. Appl Environ Microbiol **72:**5260–5265. http://dx.doi.org/10.1128/AEM.00599-06.
43. **Sinha NK, Snustad DP.** 1972. Mechanism of inhibition of deoxyribonucleic acid synthesis in Escherichia coli by hydroxyurea. J Bacteriol **112:**1321–1324.
44. **Uratani B, Lopez JM, Freese E.** 1983. Effect of decoyinine on peptidoglycan synthesis and turnover in Bacillus subtilis. J Bacteriol **154:**261–268.
45. **Cui L, Ma X, Sato K, Okuma K, Tenover FC, Mamizuka EM, Gemmell CG, Kim MN, Ploy MC, El-Solh N, Ferraz V, Hiramatsu K.** 2003. Cell wall thickening is a common feature of vancomycin resistance in Staphylococcus aureus. J Clin Microbiol **41:**5–14. http://dx.doi.org/10.1128/JCM.41.1.5-14.2003.
46. **Giesbrecht P, Kersten T, Maidhof H, Wecke J.** 1998. Staphylococcal cell wall: morphogenesis and fatal variations in the presence of penicillin. Microbiol Mol Biol Rev **62:**1371–1414.
47. **Singh P, Sengupta S.** 2012. Phylogenetic analysis and comparative genomics of purine riboswitch distribution in prokaryotes. Evol Bioinform Online **8:**589–609. http://dx.doi.org/10.4137/EBO.S10048.
48. **Lu Y, Shevtchenko TN, Paulus H.** 1992. Fine-structure mapping of cis-acting control sites in the lysC operon of Bacillus subtilis. FEMS Microbiol Lett **71:**23–27.
49. **Sudarsan N, Wickiser JK, Nakamura S, Ebert MS, Breaker RR.** 2003. An mRNA structure in bacteria that controls gene expression by binding lysine. Genes Dev **17:**2688–2697. http://dx.doi.org/10.1101/gad.1140003.
50. **Ataide SF, Wilson SN, Dang S, Rogers TE, Roy B, Banerjee R, Henkin TM, Ibba M.** 2007. Mechanisms of resistance to an amino acid antibiotic that targets translation. ACS Chem Biol **2:**819–827. http://dx.doi.org/10.1021/cb7002253.
51. **Hirshfield IN, Zamecnik PC.** 1972. Thiosine-resistant mutants of Escherichia coli K-12 with growth-medium-dependent lysl-tRNA synthetase activity. I. Isolation and physiological characterization. Biochim Biophys Acta **259:**330–343.
52. **Di Girolamo M, Busiello V, Coccia R, Foppoli C.** 1990. Aspartokinase

III repression and lysine analogs utilization for protein synthesis. Physiol Chem Phys Med NMR **22:**241–245.

53. **Cressina E, Chen L, Moulin M, Leeper FJ, Abell C, Smith AG.** 2011. Identification of novel ligands for thiamine pyrophosphate (TPP) riboswitches. Biochem Soc Trans **39:**652–657. http://dx.doi.org/10.1042/BST0390652.
54. **Trausch JJ, Batey RT.** 2014. A disconnect between high-affinity binding and efficient regulation by antifolates and purines in the tetrahydrofolate riboswitch. Chem Biol **21:**205–216. http://dx.doi.org/10.1016/j.chembiol.2013.11.012.
55. **Howe JA, Wang H, Fischmann TO, Balibar CJ, Xiao L, Galgoci AM, Malinverni JC, Mayhood T, Villafania A, Nahvi A, Murgolo N, Barbieri CM, Mann PA, Carr D, Xia E, Zuck P, Riley D, Painter RE, Walker SS, Sherborne B, de Jesus R, Pan W, Plotkin MA, Wu J, Rindgen D, Cummings J, Garlisi CG, Zhang R, Sheth PR, Gill CJ, Tang H, Roemer T.** 2015. Selective small-molecule inhibition of an RNA structural element. Nature **526:**672–677. http://dx.doi.org/10.1038/nature15542.
56. **Gruber AR, Bernhart SH, Lorenz R.** 2015. The ViennaRNA web services. Methods Mol Biol **1269:**307–326. http://dx.doi.org/10.1007/978-1-4939-2291-8_19.
57. **van Pijkeren JP, Morrissey D, Monk IR, Cronin M, Rajendran S, O'Sullivan GC, Gahan CGM, Tangney M.** 2010. A novel *Listeria monocytogenes*-based DNA delivery system for cancer gene therapy. Hum Gene Ther **21:**405–416. http://dx.doi.org/10.1089/hum.2009.022.
58. **Monk IR, Gahan CGM, Hill C.** 2008. Tools for functional postgenomic analysis of *Listeria monocytogenes*. Appl Environ Microbiol **74:**3921–3934. http://dx.doi.org/10.1128/AEM.00314-08.
59. **Christie GE, Matthews AM, King DG, Lane KD, Olivarez NP, Tallent SM, Gill SR, Novick RP.** The complete genomes of *Staphylococcus aureus* bacteriophages 80 and 80α—implications for the specificity of SaPI mobilization. Virology **407:**381–390. http://dx.doi.org/10.1016/j.virol.2010.08.036.
60. **Blount KF, Megyola C, Plummer M, Osterman D, O'Connell T, Aristoff P, Quinn C, Chrusciel RA, Poel TJ, Schostarez HJ, Stewart CA, Walker DP, Wuts PGM, Breaker RR.** 2015. Novel riboswitch-binding flavin analog that protects mice against *Clostridium difficile* infection without inhibiting cecal flora. Antimicrob Agents Chemother **59:**5736–5746. http://dx.doi.org/10.1128/AAC.01282-15.